Studies on Molecular Mechanisms of Mitosis, Meiosis and Amitosis in *Tetrahymena thermophila*

January 2014

Yasuharu KUSHIDA

Studies on Molecular Mechanisms of Mitosis, Meiosis and Amitosis in *Tetrahymena thermophila*

A Dissertation Submitted to

the Graduate School of Life and Environmental Sciences,

the University of Tsukuba

in Partial Fulfillment of the Requirements

for the Degree of Doctor of Philosophy in Science

(Doctoral Program in Biological Sciences)

Yasuharu KUSHIDA

Table of Contents

Chapter 3: Analysis of the localization and the function of *Tetrahymena* kinesin-14 during mitosis, amitosis and meiosis

Abstract

This study was performed to understand the molecular mechanisms of three distinct modes of nuclear division in ciliates, mitosis, amitosis, and meiosis. For this purpose, I first analyzed the localization of γ-tubulin (MTOC) during vegetative growth and conjugation of ciliate *Tetrahymena*. Mitosis formed bipolar spindle with thick inter-polar MT bundles. Some of γ-tubulins were left in the middle of the MT bundles. Amitosis proceeded with non-bipolar MT structure and transient astral MTs were formed during early amitosis. Amitotic MT structures were sensitive to the shut-off of γ-tubulin expression. Next, I analyzed the localization and function of MT minus-end motor, kinesin-14 (KIN14A) during nuclear division. The proper chromosome segregation during mitosis required KIN14A. However, the dynamic change of MT distribution during amitosis did not require KIN14A, and chromosome segregation during amitosis was not affected even without KIN14A. Meiotic division with characteristic elongation (called crescent) and shortening of nucleus also required KIN14A. This study clearly showed the differences of molecular mechanism among mitosis, amitosis and meiosis in the ciliate *Tetrahymena*.

Abbreviations:

AP: alkaline phosphatase

ATP: adenosine 5'-triphosphate

DAPI: 4',6-diamidino-2-phenylindole

DMSO: dimethyl sulfoxide

DYH: dynein heavy chain

EDTA: ethylene diaminetetraacetic acid

EGTA: ethylene glycol tetraacetic acid

EM: electron microscope

GCP2: gamma-tubulin accessory protein 2

GCP3: gamma-tubulin accessory protein 3

GTP: guanosine 5'-triphosphate

GTU1: gamma-tubulin 1

HA: hemagglutinin

ICT: intracilia transport

KIN1: kinesin 1

Mac: macronucleus

Mic: micronucleus

MT: microtubule

MTOC: microtubule organizing center

MTT1: metallothionein 1

OA: oral apparatus

OP: oral primordium

PAGE: polyacrylamide gel electrophoresis

PCM: pericentrosomal matrix

PVDF: polyvinylidene fluoride

SDS: sodium dodecylsulfate

SPB: spindle pole body

TGD: Tetrahymena Genome Database

TGED: Tetrahymena Gene Expression Database

γ-TuRC: gamma tubulin ring complex

γ-TuSC: gamma tubulin small complex

General Introduction

The 'nuclear dualism' is characteristic of ciliates. Ciliate species are known to contain two types of nuclei, Micronucleus (Mic) and Macronucleus (Mac). Mic is reproductive nucleus containing single set of genome, and divide by closed mitosis similar to yeast (Davidsona and LaFountain, 1975). During sexual reproduction, Mic reproduces Mac by chromosome polyploidization (Allen and Gibson, 1972) and rearrangement (Mochizuki et al., 2002). As a result, Mac contains highly polyploid chromosomes and is actively transcribed during vegetative growth. Because Mac chromosomes do not have functional centromere (Raikov, 1982), a bipolar spindle via kinetochore cannot be formed in Mac. Instead, Mac divides by apparently simple mechanism; longitudinal expansion and contraction. This type of nuclear division is called 'amitosis', which is proved to be a random segregation of chromosomes (Orias and Flacks, 1975). By observing the fine structures, non-spindle MT bundles ('pushing body') are reported inside expanding Mac (Raikov, 1982). Furthermore, anti-MT agents were found to inhibit Mac division (Tamura et al., 1969; Wunderlich and Speth, 1970). Previously, the MT structure of *Tetrahymena pyriformis*, amicronucleate species, were observed by immunofluorescence (Fujiu and Numata., 2000). So I decided to analyze the dynamics of MT during amitosis to understand how MT structure in dividing Mac can be formed and how the MT structure can produce the force to drive amitosis.

In vivo MT polymerization is usually mediated by γ-tubulin ring complex (γ-TuRC) consisted by γ-tubulin and associated-proteins. γ-tubulin has about 30% sequence identity with α/β-tubulin (Oakley and Oakley, 1989), and serves as a template of MT polymerization (Kollman et al., 2010). γ-TuRC of animal cell is mostly distributed on the surface of centrosome in a NEDD1-dependent manner (Haren et al., 2006), while some γ-TuRCs are associated on MT lattice (Goshima et al., 2008; Bouissou et al., 2009). In the ciliate *Tetrahymena*, the expression of γ-tubulin is essential for the formation of cortical MT pattering

(Shang et al., 2002a). However, the role of γ-tubulin during nuclear divisions (mitosis and amitosis) has not been well understood. In this thesis, I analyzed the localization of γ-tubulin during mitosis and amitosis to reveal the MT formation process.

In addition, to understand the mechanism of determination of the γ-tubulin distribution, I analyzed the localization and function of MT minus-end-directed motors, which can gather γ-tubulin by their MT crosslinking activity and minus-end-directed motility.

This study tries to reveal the molecular mechanism of ciliate-specific nuclear divisions by analyzing the formation process of MT and the regulation of MTs by motor protein.

Chapter 1:

Analysis of localization and function of γ-tubulin during mitosis and amitosis

Abstract

To reveal the molecular systems involved in the division of a cell and its contents during cell proliferation is one of the major subjects in cell biology. Although cytoskeletal organization during mitosis has been well studied, consensus on the molecular basis of amitosis has not been achieved. Here I adapted an immunofluorescence method and investigated the cellular localization of γ-tubulin and microtubules (MTs) in dividing *Tetrahymena*. Although the macronucleus (Mac) lacks a bi-polar spindle, γ-tubulin and MTs are specifically detected in the dividing Mac and show a marked change in the pattern of localization. First, γ-tubulin and MTs appear in whole Mac, then, γ-tubulin gathers at the center of the Mac where an aster-like structure of MTs forms. On Mac expansion, MTs associated with numerous dots of γ-tubulin are reorganized into longitudinally arranged bundles, suggesting that the mutual sliding of each filament and polymerization of MTs may induce Mac expansion. Moreover, normal Mac expansion and equal segregation of the Mac are severely disturbed when the expression of γ-tubulin is shut off. I propose that γ-tubulin-mediated MT assembly is required for Mac amitosis of *Tetrahymena*.

Introduction

Ciliates are divergent organisms from animals, plants, and fungi, and are characterized by unique cellular structures. It is well known that most ciliates have two functionally distinct nuclei: the micronucleus (Mic) contains a single set of metacentric chromosomes and is usually not transcribed, whereas the macronucleus (Mac) is actively transcribed in vegetative growing cells. These nuclei are analogous to those of reproductive and somatic cells in multicellular organisms, respectively. Mac is developed from a conjugated Mic after the mating of parental cells, and the genome becomes polyploid and fragmented into several hundred short chromosomes (Allen and Gibson, 1972). This unique nuclear system may be required for bulk gene transcription to enable the cell body to enlarge and to support the vigorous cellular activities of ciliates, which is probably advantageous for natural selection. Ciliates have evolutionarily acquired such a complicated dimorphism that the Mac is differentiated from the Mic. Coincidentally, the division process of the Mac varies between ciliate species, whereas Mic division progresses by the typical bi-polar pattern, similar to closed mitosis in yeast and fungi. The order *Karyorelictida* shows ancestral characteristics and its diploid Mac lacks the ability to divide. Therefore, the Mac is regenerated from the Mic at each cell division in this species (Raikov, 1982). With the exception of that in *Karyorelictida*, the Mac is divided in the common manner called 'amitosis'; however, some divergences seem to have arisen in the mechanism of amitosis among ciliate species. The Mac of *Blepharisma* divides with an array of cytoplasmic microtubules (MTs) on the surface of the Mac envelope. On the other hand, the Mac of *Tetrahymena* and *Paramecium* elongates with longitudinal arrangement of MTs assembled in the nucleus. Moreover, in *Paramecium*, but not *Tetrahymena*, the dividing Mac interacts with a unique structure on the cell cortex, the trichocyst, which may ensure more precise distribution of a nucleus into each daughter cell (Tucker et al., 1980). Thus, the cellular machinery for amitosis has probably been developed

through phylogenesis in each member of the ciliates and seems to be related to evolutionary differentiation of the cell architecture in each descendant. Study of the molecular mechanism of amitosis may shed light on the evolutionary process of nuclear dimorphism and the life history of ciliates.

The *Tetrahymena pyriformis* ciliate grows asexually because of a lack of a Mic; MTs seem to play an important role in longitudinal expansion of the Mac ahead of its division (Williams and Williams, 1976). The Mac is passively segregated in an asymmetric manner by contraction of the cleavage furrow in cells treated with colchicine, an inhibitor of the polymerization of tubulin (Tamura et al., 1969; Wunderlich and Speth, 1970). Electron microscopic (EM) studies showed the organization of MTs in and around a dividing Mac, which is quite different from a bi-polar spindle, a common structure for the nuclear division of animal and fungal cells (Ito et al., 1968; Tamura et al., 1969; Wunderlich and Speth, 1970). The observation of MT assembly using fluorescence microscopy showed that Mac MTs change their distribution and arrangement according to the longitudinal expansion and fission of Mac (Fujiu and Numata, 2000).

γ-tubulin, approximately 30% identical in amino acid sequence to α- and β-tubulin (subunits of MT) (Oakley and Oakley, 1989), plays an essential role in initiating MT assembly reference. This protein is associated with accessory proteins Spc97 (GCP2) and Spc98 (GCP3) and forms γ-tubulin small complex (γ-TuSC) (reviewed by McKean et al., 2001; Wiese and Zheng, 2006). Multiple γ-TuSCs can form a ring structure, which mimics the end of an MT, and serves as a microtubule template for polymerization (Kollman et al., 2010). In metazoa, other proteins assemble with γ-TuSC into a γ-tubulin ring complex (γ-TuRC), which probably enables more elaborate spatiotemporal control of MT organization. γ-TuRC is localized around the centrosome of animal cells; therefore, the minus end of MT is oriented towards the center and the plus end towards the exterior of the cell. This polarized organization of MTs is

indispensable for intracellular architecture and membrane traffic. In addition, γ-TuRC controls the plus-end dynamics of MT by associating with the wall of MT filament (Bouissou et al., 2009). γ-tubulin has recently been found to be important for MT nucleation from a side of the existent MT filament (Murata et al., 2005) and for augmentation of MTs within the mitotic spindle (Goshima et al., 2008). In *Tetrahymena* cells, γ-tubulin is detected at several MT-organizing centers including these in dividing Mac (Shang et al., 2002a; Joachimiak et al., 2007). Depletion of γ-tubulin was found to markedly alter cortical MT structures, and among γ-tubulin localizing regions in the cell, basal bodies were most sensitive to γ-tubulin depletion (Shang et al., 2002a).

To further understand the molecular mechanism that controls the spatiotemporal organization of Mac & Mic MTs, here I investigated the detailed cellular localization of γ-tubulin and associated MTs, and evaluated the effect of γ-tubulin depletion on Mac & Mic divisions using a shut-off strain for gene expression. The results led me to conclude that Mac MTs engaged in amitosis are organized in a manner dependent on γ-tubulin.

Materials and Methods

Cell strain and media

To investigate the organization of MTs and the effect of cold treatment or nocodazole on this in *T. thermophila*, CU428 strain cultured in SPP (1% proteose peptone, 0.1% yeast extract, 0.2% D-glucose, 0.003% Fe (III)-EDTA) was used.   Strain cTTMGHA (Shang et al., 2002a), kindly donated by Prof. Martin A. Gorovsky (University of Rochester), cultured in SPP with 0.25 µg/ml $CdCl_2$, was used to co-stain MTs and γ-tubulin or for the shut-off experiment of γ-tubulin. The concentration of $CdCl_2$ was one-quarter of that of the previous report (Shang et al., 2002a), which does not cause any defect in the growth rate, the number of food vacuoles or the chromatin mass in the Mac (Piccinni et al., 1987).

Fluorescence microscopy

Staining of MTs was performed according to the previously described method (Fujiu and Numata, 2000).   Cells were treated with mouse anti-chicken α-tubulin antibody (CalBiochem) (1:150 dil.) at 4°C overnight. After washing, FITC-conjugated goat anti-mouse IgG antibody (TAGO) (1:150 dil.) treated was at room temperature for 6 h.   Nuclear DNA was stained with DAPI (4',6-diamidino-2-phenylindole; final conc. 1 µg/ml).

Staining of γ-tubulin was mainly performed according to the method of Gaertig and Fleury (1992) with some modification.   Cells were washed once with PiEM (10 mM Pipes, 10 mM EGTA, 5 mM $MgSO_4$, pH 6.9) (Nakagawa et al., 2008) and permeated by incubation in PiEM with 0.5% TritonX-100 and 10 µM taxol for 3 min. After washing once with PiEM, cells were fixed in PiEM with 2% formaldehyde.   After 1 h, cells were washed twice with PEM (0.145 M NaCl, 7.4 mM Na_2HPO_4-$12H_2O$, 2.6 mM NaH_2PO_4-$2H_2O$, 2 mM EGTA, 5 mM $MgSO_4$, pH 7.2) (Fujiu and Numata, 2000) and air-dried on a cover slip.

Cells were then pretreated with PEM with 3% bovine serum albumin (BSA) and 0.1%

Tween 20 for 30 min and incubated with mouse anti-α-tubulin antibody (1:250 dil.) and rat anti-HA antibody, clone 3F10 (Roche Applied Science) (1:250 dil.) for 1 h. After washing with PEM and with 3% BSA and 0.1% Tween 20 three times, cells were incubated with Alexa-555-conjugated goat anti-mouse IgG antiserum and Alexa-488-conjugated goat anti-rat IgG antiserum (Molecular Probes) (each 1:250 dil.) for 1 h. DNA was stained with DAPI (final conc. 1 μg/ml).

For observation, a confocal laser microscope (Carl Zeiss LSM510 with an alpha Plan-Fluar 100×lens (N.A. 1.45)) or the Delta Vision deconvolution microscope system (Applied Precision; Olympus IX71 with an UPlanApo 100×lens (N.A. 1.35)) was used.

Nocodazole treatment

Nocodazole (final conc. 30 μM) or an equal volume of DMSO solvent (control) was added to the cell culture and incubated for 10 min at 30°C. Cells were then processed for observation with a fluorescence microscope (Olympus BX-51 with an UPlanSApo 40×lens (N.A. 0.95)).

Western blotting

To examine the protein level of γ-tubulin, 10^4 cells were centrifuged, mixed with 40 μl sampling buffer (62.5 mM Tris-HCl, 2% SDS, 5% sucrose, 0.002% bromophenol blue, 10% 2-mercaptoethanol, pH 6.8), and incubated at 95°C for 5 min. Samples were subjected to SDS-10% PAGE and transferred to a PVDF membrane. The membrane was pretreated with TTBS (20 mM Tris-HCl, 0.9% NaCl, 0.05% Tween 20, pH 7.5) containing 1% skim milk for 1 h, and incubated with rabbit anti-HA antibody (Bethyl Laboratories, Inc.) (1:1000 dil.) or mouse anti-α-tubulin antibody (1:1000 dil.) for 2 h. After washing three times with TTBS containing 1% skim milk (each for 10 min), the membrane was incubated with alkaline

phosphatase (AP)-conjugated anti-rabbit IgG antibody (Santa Cruz Biotechnology) or AP-conjugated anti-mouse IgG antibody (Biosource International) (each 1:1000 dil.) for 1 h. After washing three times with TTBS and three times with TTBS without Tween 20 (each for 10 min), AP was detected by incubation with BCIP/NBT solution (Kirkegaard & Perry Laboratories, Inc.).

Results and Discussion

γ-tubulin accumulates to spindle poles of inter-polar MT bundles during Mic mitosis

I first observed the organization of MTs during cell division in *T. thermophila* using a fluorescence microscope (Fig. 1). Interphase Mic was observed in the depression in the Mac (Fig. 1a'). γ-tubulin was detected as multiple dotted fluorescent signals on the surface of the Mic (Fig. 2a). At the beginning of the division phase, an oral primordium (Fig. 1b, OP) was formed at the posterior of the prospective division furrow. Several MT bundles were appeared in the Mic while the Mic was attached on the Mac (Fig. 2b, arrows). These MT bundles were already shaped like a 'spindle' which outlines the shape of the Mic. γ-tubulin was localized at the both ends of MT bundles (Fig. 2b, arrowheads) while multiple dotted signals were also detected along the MT bundle. When the shape of the Mic became bipolar spindle, while some fluorescent signals of γ-tubulin were still distributed along MT bundle, the accumulation of γ-tubulins were detectable on spindle poles (Fig. 2c, arrowheads). The Mic spindle of this stage corresponds to metaphase to anaphase A of animal cells. The MT bundles in this stage (Fig. 2c, arrows) are likely to work as 'inter-polar MTs' which bridges opposite spindle poles. Several discontinuous MTs were observed in the middle of spindle (Fig. 2c, yellow arrowhead), which seems to be kinetochore MTs (k-fibers) connecting chromosomes to each spindle pole. Later, the Mic is detached from the Mac and proceeds to the phase of chromosome segregation. When the segregation of the Mic chromosomes was almost completed (Fig. 2d; corresponding to anaphase B of animal cells), multiple signals of γ-tubulin appeared in the middle of Mic spindle (Fig. 2d, arrowheads), which suggests new MT polymerization during expansion of the spindle. When the Mic division is completed, the Mic was shaped like 'dumbbell' since two daughter Mics were connected by spindle MTs (Fig. 2e). γ-tubulin was distributed on the surface of the two daughter Mics (Fig. 2e, arrowheads). Although γ-tubulin seemed to be detached from spindle MTs, the signals of γ-tubulin preferentially distributed at the both ends

of the Mic where spindle poles were existed.

The distribution of γ-tubulin during the Mic mitosis suggests new mechanism of mitotic spindle formation. Generally, mitotic spindle is organized by astral MTs nucleated from MTOC like centrosomes of animal cell (reviewed in Tanenbaum and Medema, 2010) or spindle pole bodies (SPBs) of yeast (reviewed in Winey and Bloom, 2012). Astral MTs are crosslinked by the kinesin-5 (Eg5) motor protein and forming anti-parallel MT bundles. Duplicated two MTOCs like centrosomes are originally positioned side-by-side. Accompanying anti-parallel MT-bundle-formation driven by kinesin-5, two MTOCs migrate to opposite ends of spindle and are interconnected by their astral MT. Eventually, MTOCs become spindle poles in animal cell. In contrast, astral MTs were never observed throughout the Mic mitosis in *Tetrahymena*. Instead, inter-polar MT bundles were formed at the beginning of *Tetrahymena* mitosis (Fig. 2b, arrows). Since some γ-tubulins were positioned at the ends of these MT bundles (Fig. 2b, c, arrowheads), *Tetrahymena* γ-tubulin may aggregate by itself (directly or indirectly) and polymerize bundled MTs. Some γ-tubulin dots were distributed along the inter-polar MT bundles and some of them were eventually detectable to the both ends of spindle to form spindle poles. This means that minus ends of MTs were assorted to the spindle poles probably by mutual sliding of MTs to form spindle poles. Surprisingly, kinesin-5 family gene does not exist in the genome of *Tetrahymena* or *Paramecium* (discussed in chapter 3), another well-known ciliate. Alternate MT plus-end motor is not reported yet in ciliates. New mechanism of mitotic spindle formation observed in *Tetrahymena* possibly gives an explanation why ciliate enables to achieve bipolar spindles without major mitotic crosslinker stabilizing anti-parallel MT bundle in the middle of spindle. Analysis of the distribution of MT plus-ends along mitotic inter-polar MT bundles of *Tetrahymena* would be very informative for further discussion.

Mac MTs are dynamically reorganized in amitosis

Before cell division, a few short scattered MTs were detected in the Mac whereas a fine meshwork of MTs was organized throughout the cytoplasm (interphase, Fig. 1a). When the Mic spindle appeared, randomly arranged MTs appeared in the Mac (stage 1, Fig. 1b, arrow). Following spindle elongation in the Mic (Fig. 1c, arrowhead), which corresponds to anaphase B of animal cells, an aster-like structure of MTs was observed in the center of the Mac (stage 2, Fig. 1c, arrow). At almost the same time as the Mic division was completed, this aster-like structure was reorganized into long MTs and arranged parallel to the longitudinal axis of the cell, and the Mac expanded ahead of its division (stage 3, Fig. 1d). MTs in the longitudinal array of expanding Mac were stained stronger than cytoplasmic MTs, suggesting that the bundling of MTs might be induced along with Mac expansion. The MT bundles in dividing Mac of *T. pyriformis* have been already observed by EM (Falk et al., 1968). It is possible that proteins laterally associated with MTs or kinesin-like motors are involved in the process. In advance of the formation of cleavage furrows for cytokinesis, Mac MTs were reduced in the middle region of half parts in the dividing Mac whereas MTs remained in the dividing region of the Mac (stage 4, Fig. 1e). At this stage, MTs on the periphery of the Mac became prominent, which looked like eyeglasses (Fig. 1e). A non-staining region was present in the middle of the MTs located in the dividing region of the Mac at the completion of Mac division (stage 5, Fig. 1f). This may be because of Mac DNA left in the central region (see stage 5 cell shown in Fig. 1) or too tight bundling of MTs to allow penetrating of antibodies. Detailed study with EM is needed for further clarification.

With cold treatment, the vast majority of the cytoplasmic MTs disappeared within five minutes, whereas stable MTs in cilia and cortical structures remained (Fig. 3). Interestingly, Mac MTs also remained (Fig. 3, arrow, Table I), suggesting that Mac MTs are stabilized, possibly by the associated proteins.

14

In addition, I noticed that the punctated distribution of Mac DNA became prominent and that DAPI-negative spaces appeared in the center of the Mac in the division phase (Fig. 4). This observation implies that the chromatin can be assembled along the Mac division.

MT structure is required for Mac division

Anti-MT drugs affect Mac division in *Tetrahymena* cells (Wunderlich and Peyk, 1969; Stone, 1968). However, MT structure under such Mac-division-affecting conditions was not well observed. To address the organization of MTs in the dividing Mac, I treated *T. thermophila* cells with nocodazole, an anti-polymerization agent for MTs, at a final concentration of 30 μM for 10 min at 30°C.   As a result, MTs disappeared from the dividing Mac and cytoplasm, whereas MTs in the cilia and cell cortex including oral apparatus (OA) remained (100%, n=19, Fig. 5). Next I examined segregation of the Mac of cells treated with 30 μM nocodazole for 30 min (Table II). Treated cells displayed unequal segregation of Mac DNA and incomplete expansion of the Mac. Therefore, MT structures are required for expansion and binary fission of the Mac.

Localization of γ-tubulin in dividing Mac

To address the mechanism of MT formation in the Mac during cell division, I investigated the localization of γ-tubulin using a strain, cTTMGHA (Shang et al., 2002a), whose sole γ-tubulin gene, *GTU1*, was replaced with *GTU1-HA* expressing HA-tagged protein under the control of a Cd^{2+}-inducible *MTT1* promoter.   In agreement with the original report (Shang et al., 2002a), γ-tubulin, detected by anti HA antibodies, was localized to basal bodies on the cell surface throughout the cell cycle (Fig. 6), which was not detectable in negative control with wildtype strain (data not shown).   In addition, a small amount of γ-tubulin was detected in the cytoplasm.   At the beginning of the division phase, γ-tubulin was detected at the oral

primordium and in the pole region of spindles engaged in Mic division (Fig. 6, stage 2). Accumulation of γ-tubulin in the center of Mac was also found. By determining γ-tubulin distribution in Mac at the early division phase, which was assessed by the shape of the dividing Mic, I observed the behavior of γ-tubulin and MTs in detail (Fig. 7). Before Mic DNA segregation, γ-tubulin appeared as fine dots associated with randomly arranged MTs in the Mac. These dots increased in number and accumulated in the center of the Mac as Mic DNA divided. Thus, the formation of MTs seems to start in the whole nucleoplasm and then strengthen at the center. Alternatively, MTs associated with γ-tubulin may gradually migrate to the center; these possibilities are not mutually exclusive. After completion of Mic DNA segregation in the late division phase, longitudinal expansion of the Mac took place (Fig. 6, stage 3). Intense signal of γ-tubulin was dispersed in expanding Mac, suggesting that the arrays of MTs may be rearranged by mutual sliding of anti-parallel MT. In contrast to its accumulation at the pole region of Mic spindle (see stage 2 in Fig. 6), γ-tubulin did not show polarized localization in expanding Mac. This distribution indicates that minus ends of MTs do not localize at particular region in expanding Mac, though γ-tubulin possibly localizes along the side of MT filaments. In stage 4, γ-tubulin-associated MTs were crowded in the middle part of the dividing Mac.

γ-tubulin is essential for Mac division

Next, I addressed the effect of γ-tubulin depletion on the organization of MTs in Mac division using the cTTMGHA strain. The expression level of GTU1-HA was significantly reduced after the washout of Cd^{2+} from the medium (Fig. 8a). No significant change of mitotic index was found (data not shown), suggesting that the cell cycle progresses in this condition. At 14 h after the washout, abnormally thick bundles of MTs were frequently seen in mitotic cells (Fig. 8b, 14 h, arrow) but not in interphase cells (data not shown). These MT bundles

seem to surround the surface of the Mac, though I cannot strictly tell whether these bundles exist on outside or inside of Mac. Detailed study with EM is needed for further clarification. At 17 h after the washout, these bundles became obvious while MTs were absent in the middle of the Mac (Fig. 8b, 17 h). Accompanying a defect in organization of MTs in the Mac, symmetrical distribution of the dividing Mac was severely affected (Fig. 8c, Table III). At 14 h, cells with asymmetrically elongating Mac ("Unequal") were produced. At 17 h, Mac elongation was strongly suppressed ("Absent"). Moreover, it was often found that the Mac was passively divided by cell cleavage only when the Mac was positioned in the middle of dividing cells ("Incomplete"). The organization of cytoplasmic MTs in mitotic cells was unlikely to be affected by the shut-off of γ-tubulin (Fig. 8b). This means that the pulling force by cytoplasmic MTs alone seems to be insufficient for full expansion of the Mac. Therefore, I concluded that the function of γ-tubulin-dependent nuclear MTs was required for Mac division. Remarkably, a similar defect in Mac division was reported in a paclitaxel-hypersensitive mutant strain of *T. thermophila* (Smith et al., 2004); with treatment of paclitaxel, Mac was associated with abnormally robust bundles of MTs, which severely affected the normal segregation of Mac. Considering the close resemblance of a phenotype with strong stabilization of MTs by taxol, depletion of γ-tubulin may strongly decrease the frequency of *de novo* polymerization of MTs and may secondarily induce hyperelongation of a small number of MTs. However, at this stage, I do not know why abnormally elongated MTs surround Mac.

In addition, it has been well examined that the onset of cytokinesis is delayed when nuclear division is affected in yeast and animal cells. In contrast, in *T. thermophila*, cytokinesis progressed in spite of abnormal Mac division induced by the shut-off of γ-tubulin (Fig. 8c, Table III).

Meanwhile, as in a previous report (Shang et al., 2002a), a spindle in the dividing Mic was normally shaped before and after γ-tubulin depletion (Fig. 8b). The percentage of Mic-dividing

cells was not significantly changed (data not shown), which indicates that Mic division was not arrested at a certain stage. Therefore, bi-polar spindle assembly and its function seem to be less sensitive to γ-tubulin depletion than organization of nuclear MT in the Mac of a dividing *T. thermophila* cell. This is presumably because the lower turnover rate of Mic γ-tubulin compared with that of Mac γ-tubulin, as Shang et al. (2002a) found that a significant amount of γ-tubulin localized to Mic remained after 30 h of γ-tubulin depletion while its localization on basal bodies and Mac disappeared. Since γ-tubulin depletion is fatal to cell proliferation mainly because of disorganization of cortical MT patterns as well as abnormal Mac segregation, it is impossible to evaluate the significance of γ-tubulin depletion on Mic mitosis through this approach.

Conclusions

Tetrahymena mitosis turns out to have a very different mechanism of bipolar spindle formation, compared with animal cells, according to the distribution of spindle MT and γ-tubulin. Mic mitosis starts with the formation of thick inter-polar MT bundles. Most of γ-tubulin is self-accumulated before MT polymerization and remaining γ-tubulins are assorted to both spindle poles by mutual sliding of MTs to achieve spindle bipolarity. Since Mic MTs are stable under nocodazole treatment, unknown MT-associating protein may stabilize these MT bundles during mitosis.

The hypothetic model of Mac amitosis based on this study is illustrated in Fig. 9. At the beginning of the division phase, γ-tubulin is accumulated in the Mac, and the polymerization of MTs takes place in a random orientation throughout the Mac (stage 1). Then, both MTs and γ-tubulin gradually concentrate at the center of the Mac (stage 2). This accumulation of γ-tubulin-associated MTs may resemble minus-end focusing at the polar region of bi-polar spindle assembled with noncentrosomal MTs. Motor proteins such as dynein and other proteins associated with the minus end of MTs may function in this step. In addition, γ-tubulin accumulated at the center of the Mac can induce the further polymerization of MTs to reinforce formation of a radial MT structure extending to the periphery of the Mac. Ahead of Mac expansion, MTs are reorganized into an array parallel to the long axis of the cell, possibly because of mutual sliding of each filament by motor proteins (stages 3 and 4). Although the mechanism for producing force for Mac expansion is still unknown, additional polymerization of MTs and bundling of the filaments also contribute to the enlargement of the MT structure in the Mac. With the achievement of full expansion of the Mac, depolymerization of MTs seemed to be triggered in nucleoplasm while bundling of MTs seemed to progress in the narrow region of the dividing Mac (stage 5). Generally, MT is likely to be absent or not detected from the very center of the contracting Mac.

19

The dynamic change of the distribution of γ-tubulin during mitosis and amitosis encourages the analysis of MT minus-end regulators such as cytoplasmic dynein and kinesin-14. Details of the analysis will be shown in chapter 3 of this thesis.

Chapter 2:

Analysis of localization of γ-tubulin during conjugation

Abstract

During sexual reproduction of ciliates, germline Mic undergoes a series of nuclear division and nuclear fusion to finally develop new somatic Mac of new generation. In prophase of meiosis I, Mic elongates to form a 'crescent' requited for the pairing of homologous chromosomes. Later, the crescent shortens to form bipolar meiotic spindle. After meiosis, one out of the four meiotic products is "selected" to undergo mitosis to produce two genetically identical pronuclei; one of each pair of pronuclei is then exchanged between the conjugating cells and fused with the stationary pronuclei in the recipient cell. Although post-meiotic nuclear selection requires polymerization of microtubules (MTs), the molecular mechanism behind this process remains unknown. Here, I analyzed the localization of the main component of the MT-organizing center, γ-tubulin, in conjugating *Tetrahymena* to understand the process of MT polymerization during meiotic and post-meiotic reproductive stages. I found that the bipolarity of meiotic spindle is established during the shortening of crescent in meiosis I. Moreover, I found that γ-tubulin selectively accumulated on the surface of a single meiotic product, and that astral cytoplasmic MTs extended from this selected meiotic product, suggesting that γ-tubulin organized polymerization of the astral MTs. Because the astral architecture of nucleus-derived MTs was most conspicuous around the pronuclei before pronuclear fusion, I consider that these astral MTs are likely to be involved in reducing the distance between pronuclei. My study suggests that the selected meiotic product is distinguished from the non-selected products by an accumulation of γ-tubulin, and that the astral MTs polymerized from the surface of pronuclei are important for pronuclear migration.

Introduction

Sexual reproduction of ciliate *Tetrahymena* (called conjugation or mating) is aimed to produce new macronucleus (Mac) as the result of sequential nuclear divisions and fertilization of germline micronucleus (Mic) (intensively reviewed in Cole and Sugai, 2012). Parental Mac expresses all the necessary genes required for the proceeding of conjugation, and finally degraded by apoptosis-like mechanism with the completion of new Mac differentiation (Akematsu et al., 2010, 2014).

When a matured *Tetrahymena* cell is incubated under low-nutrient condition, the mating activity of the cell will be expressed. By mixing starved cells belonging to two complemental mating types, cells will start mating by connecting cell cortex of anterior part of the cell. Germline pronuclei are formed in each mating cells, and one out of the two pronuclei is exchanged through protoplasmic connection positioned at anterior end of the cell. After fertilization between self and non-self pronuclei, new Mac and Mic are differentiated by post-zygotic nuclear divisions. Two mating cells will be separated and each of them starts growing as the sexually immature cells of new generation.

There is no G1 phase in the cell cycle of *Tetrahymena* Mic. Because the Mic chromosomes are duplicated during anaphase of mitosis, nuclear phase of interphase Mic is always 4C (Cole and Sugai, 2012). When the *Tetrahymena* conjugation is induced, the Mic starts meiosis I without DNA duplication. The Mic is detached from the depression of the Mac and start to elongate. The elongating Mic during ciliate conjugation is called 'crescent', which corresponds to 'bouquet' seen in meiosis of animal cells (Raikov, 1982). This specific phase of meiosis is known as the period of paring of homologous chromosomes to form a bivalent chromosome. In fission yeast, pairs of homologous chromosomes are 'shaken' by oscillatory movement of nucleus driven by MT and motor protein (Ding et al., 1998). This 'horse-tail movement' promotes the formation of bivalent chromosome during yeast meiosis. During *Tetrahymena*

'crescent', Mic chromosomes are highly decondensed and their complete paring is achieved only when crescent become fully elongated (Loidl and Scherthan, 2004; Mochizuki et al., 2008; Loidl and Mochizuki, 2009; Loidl et al., 2012). After paring of homologous chromosomes is finished, chromosomes are condensed rapidly and gathered near one end of the crescent. This is when crescent starts to shorten and finally a bipolar meiotic spindle is formed.

Since the treatment of anti-MT drugs disturbs almost every step of conjugation, MT polymerization is considered to be essential for progression of the conjugation stages (Kaczanowski et al., 1985, 1991; Hamilton et al., 1988). Fluorescence microscopy of MT during conjugation shows that MTs in elongated crescent are somehow collected during shortening of the crescent and those MTs form meiotic spindle with thick bundles of MTs (Gaertig and Fleury, 1992). It is tempting to imagine that MT bundles of the crescent are gathered by mutual sliding to form the meiotic spindle. The mechanism of meiotic spindle formation remains unknown in *Tetrahymena*.

Preceding fertilization, one nucleus is 'selected' among the four meiotic products, and forms two pronuclei by gametogenic mitosis. One of the two pronuclei is exchanged with pronucleus of the partner cell through the protoplasmic connection for successful fertilization. MT distribution shown by Gaertig and Fleury (1992) reveals that the 'selected' post-meiotic nucleus is preferentially labelled with MTs, and MTs are persistent during later stages, namely gametogenic mitosis, nuclear exchange, fertilization and post-zygotic divisions. During determination of one gametic nucleus from the four meiotic products, one nucleus is pushed to conjugational plane (Cole and Sugai, 2012). This movement of nucleus is considered to be important for nuclear selection though its molecular mechanism is never proven. Since MTs are only accumulated on selected gametic nucleus produced by meiosis, it is important to address the mechanism of MT polymerization during nuclear selection. In fact, the expression

of γ-tubulin is essential for the formation of a proper MT structure in dividing Mac (Chapter 1; Fig. 8) and for cortical MT patterning (Shang et al., 2002a), implying that γ-tubulin is involved in MT formation during conjugation. Indeed, according to the *Tetrahymena* functional genomics database (TetraFGD; http://tfgdgb.ihb.ac.cn/) (Xiong et al., 2013), the expression level of γ-tubulin during conjugation (especially in the post-meiotic phase) is about 10 times that observed during the vegetative growing phase.

In this chapter, I analyzed the localization of γ-tubulin by indirect immunofluorescence to understand how the bipolar spindle is organized after elongation and shortening of the 'crescent' Mic. Besides, to shed light on the mechanism that limits MT polymerization to the selected meiotic product and its derivatives, I also address the γ-tubulin localization during gametogenic mitosis, nuclear exchange, fertilization and post-zygotic divisions to understand the importance of MT polymerization on nuclear 'selection'.

Materials and Methods

Cell strain and media

To investigate the distribution of γ-tubulin during conjugation of *Tetrahymena*, strain CU428 was crossed with strain cTTMGHA (Shang et al., 2002a), which expresses HA-tagged *Tetrahymena* γ-tubulin under the control of a cadmium-ion inducible promoter (*MTT1*). The strain cTTMGHA and the strain CU428 were kindly donated by Prof. Martin A. Gorovsky (University of Rochester) and Prof. Jacek Gaertig (University of Georgia), respectively. Both strains were cultured in SPP medium (1% (w/v) proteose peptone, 0.1% (w/v) yeast extract, 0.2% (w/v) D-glucose, 0.003% (w/v) Fe (III)-EDTA). One microgram per milliliter of $CdCl_2$ was added to the cTTMGHA culture (Shang et al., 2002a). The cells were starved in 10 mM Tris-HCl (pH 7.5) at 30°C overnight before mating.

Fluorescence microscopy

To induce conjugation, equal numbers of starved cells from each strain (~10^5 cells/mL) were mixed and incubated at 30°C. Cells were sampled from 1.5 to 9.5 h at intervals of 15 min and fixed in accordance with the methods described in Chapter 1. Anti-α-tubulin antibody and anti-HA antibody were used to detect MTs and a HA-tagged recombinant γ-tubulin (GTU1-HA) expressed in cTTMGHA, respectively. Fixed cells were treated with mouse anti-chicken α-tubulin antibody (Calbiochem, Darmstadt, Germany; 1/300 dilution) and rabbit polyclonal anti-HA antibody (Bethyl Laboratories, Montgomery, TX; 1/300 dilution) at room temperature overnight. After being washed, the cells were incubated with FITC-conjugated goat anti-mouse IgG antiserum (TAGO, Burlingame, CA; 1/300 dilution) and rhodamine-conjugated goat anti-rabbit IgG antiserum (Kirkegaard & Perry Laboratories, Gaithersburg, MD; 1/300 dilution) for 6 h at room temperature. DNA was stained with 4',6-diamidino-2-phenylindole (DAPI; final concentration, 1 µg/mL). Cells were observed

under a confocal laser scanning microscope (Carl Zeiss, Oberkochen, Germany, LSM700) with an alpha Plan-Apochromat 100× lens with the numerical aperture of 1.46. The conjugational stage of each pair of cells was identified in reference to the reported observations of DNA (Cole and Sugai, 2012) and MT (Gaertig and Fleury, 1992) distributions.

Results

γ-tubulin is accumulated on one end of Mic at the start of elongation of 'crescent'

When the Mic is detached from the Mac, several dotted fluorescent signals of γ-tubulin were detected on the surface of the Mic (Fig.10a, arrowhead). At the time of beginning of crescent elongation, γ-tubulin was strongly accumulated at one end of the Mic (Fig. 10b, arrowhead) and rapidly produced a lot of MTs in one direction (Fig. 10b, arrow). During expansion of the crescent, a layer of MTs is observed using EM (Wolfe et al., 1976; Suganuma and Yamamoto, 1992). This polarized group of MTs is most likely to produce force required for the crescent elongation.

γ-tubulin disperses over fully elongated Mic 'crescent'

As elongation of crescent proceeds, most of γ-tubulin dots gradually dispersed on MT bundles set free from one end of the crescent, while some γ-tubulin dots stayed at the same position (Fig. 10c, arrowhead). When the crescent completes elongation, its length was about two times of the length of the cell body (Fig. 10d, arrow). At that time, γ-tubulin dots distributed uniformly along full length of the crescent, and all γ-tubulin was released from one end of crescent (Fig. 10d).

γ-tubulin dots accumulated at both ends of the shortening crescent

After crescent fully elongates and Mic chromosomes finish homologous pairing, the chromosomes start condensing toward one side of the crescent (Fig. 10e, asterisk). MT bundles positioned in chromosome-free region of the crescent are rapidly bundled together to form thicker MT bundles, and the shortening of the crescent started (Fig. 10e, arrow). These thick MT bundles became thicker and shorter. The dotted signals of γ-tubulin became obvious on this thick bundle of MTs (Fig. 10e, arrowhead). As shortening of the crescent proceeds,

27

γ-tubulin accumulated on the end of the MT bundle (Fig. 10f, 10f' arrowhead), namely the end of the shortening crescent. Accumulation of γ-tubulin is also observed on the other end of crescent MTs when the length of the crescent become close to that of the meiotic spindle (Fig. 11a, arrowheads). Finally, all the MTs were gathered within about one third of length of cell body to form a meiotic spindle. γ-tubulin is clearly detected on both ends of the thick MT bundles, showing bipolarity of the spindle (Fig. 11b, arrowheads). The dotted signals of γ-tubulin were detected of daughter nuclei of meiosis I (Fig, 11d, arrowheads), and γ-tubulin accumulated again on the spindle poles of meiosis II (Fig. 11e, arrowheads).

Abundant γ-tubulin accumulated on the surface of the selected meiotic product

In *Tetrahymena*, among the four nuclei produced by meiosis (Fig. 12A, arrowheads), only one nucleus becomes closely attached to the conjugation plane positioned at the anterior part of the cell (Fig. 12B, large arrowheads). This phenomenon has been termed nuclear "selection" (Cole and Sugai, 2012). By immunohistochemistry, I observed that, at the time of nuclear selection, γ-tubulin coated the whole surface of the selected nucleus (Fig. 12B, large arrowheads), and astral MTs extended from the selected nucleus to the cytoplasm (Fig. 12B, arrows), suggesting that γ-tubulin promoted polymerization of the astral MTs. Notably, many γ-tubulin accumulated at the conjugation junction during nuclear selection (Fig. 12B, small arrowhead). The selected gametic nucleus and its derivatives were constantly coated with abundant γ-tubulin during the later stages of conjugation, namely gametogenic mitosis, pronuclear migration, pronuclear exchange, fertilization, and post-zygotic division (Fig. 12C, 12D, 12E, 12F, 12G, 13A, 13B, 13C, large arrowheads).

Astral MTs formed from γ-tubulin coating the migrating pronuclei

Two gametic pronuclei are formed by mitosis of the selected meiotic product, in a process

called gametogenic mitosis (Cole and Sugai, 2012; Fig. 12C, arrows). I observed that, during anaphase of gametogenic mitosis, γ-tubulin accumulated strongly on both daughter pronuclei (Fig. 12D, large arrowheads). Whereas the majority of the fluorescent signal for MTs labeled the mitotic spindle that connected the daughter pronuclei (Fig. 12D, arrow), some astral cytoplasmic MTs were observed around the anterior daughter pronucleus (Fig. 12D, small arrowhead). The posterior daughter pronucleus was easily distinguished from the remaining, unselected, meiotic products because the pronucleus was strongly labeled with γ-tubulin (Fig. 12D, lower large arrowhead).

After being severed from the spindle MTs, the posterior pronucleus starts to move to the anterior end of the cell, where fertilization occurs (Ray, 1956; Martindale et al., 1982; Cole and Sugai, 2012; Fig. 12E, large arrowhead). I observed that, when the spindle MTs disappeared, clear astral cytoplasmic MTs were produced from the γ-tubulin surrounding the migrating posterior pronucleus (Fig. 12E, arrow), as well as from the anterior pronucleus (Fig. 12E, small arrowhead).

During pronuclear migration, the anterior pronucleus is exchanged with the pronucleus of the partner cell. Electron microscopic studies report that an MT "basket" seems to push the pronucleus against the conjugational plane to enable successful transfer of the nucleus (Orias et al., 1983; Cole, 2006). I detected abundant γ-tubulin on this basket (Fig. 12H, arrowhead) and polymerization of abundant astral cytoplasmic MTs from the basket (Fig. 12H, arrow). These results suggest that γ-tubulin promotes the polymerization of astral cytoplasmic MTs from the MT basket surrounding the anterior pronucleus.

γ-tubulin coating the fertilized nucleus and daughter nuclei of post-zygotic division

The posterior pronucleus that arrives at the anterior end of the cell fuses with the anterior pronucleus transferred from the partner cell to become one fertilized nucleus (Cole and Sugai,

2012; Fig. 12G, arrow). I detected γ-tubulin on the transferred anterior pronuclei (Fig. 12F, upper large arrowhead) even after nuclear exchange, though most γ-tubulin was detected at the cell junction (Fig. 12F, asterisk). After fertilization, the spindle-shaped fertilized nucleus was labeled strongly with γ-tubulin (Fig. 12G, arrowhead).

The first two post-zygotic divisions produce two Mic and two new Mac (Cole and Sugai, 2012). I observed that during the first post-zygotic division, γ-tubulin was located all over the MTs (Fig. 13A, arrowhead) and accumulated on the surface of the daughter nuclei at anaphase (Fig. 13B, arrowheads) and after severed from the spindle (Fig. 13C, large arrowheads). This pattern of γ-tubulin localization is similar to that observed at gametogenic mitosis (Fig. 12D, large arrowheads). The presence of abundant γ-tubulin coating the nuclei is no longer seen after the second post-zygotic division (Fig. 13D, arrowheads).

γ-tubulin inside swelling new Macs

After the second post-zygotic division, the two anterior daughter nuclei differentiate to form new Macs and the two posterior nuclei become the two new Mics (Cole and Sugai, 2012). I observed that when the MT spindle of the second post-zygotic division disappeared, the network of cytoplasmic MTs was highly augmented (Fig. 13E, 2nd left panel). Some γ-tubulin molecules were briefly detected in the parental Mac (Fig. 13E, arrow), and scattered MTs were formed in the parental Mac (Fig. 13E, small arrowhead). These γ-tubulin molecules and MTs disappeared quickly when the parental Mac started to condense for degradation (Fig. 13F, arrow). Several dotted signals of γ-tubulin were detected in both of the new Macs (Fig. 13E, F, large arrowheads) as well as in both of the new Mics (Fig. 13F, small arrowheads). The γ-tubulin signals of new Macs increased (Fig. 13G, arrowheads and Fig. 13H, arrows) and some dotted signals of MTs were detectable in the new Macs when they swelled (Fig. 13H, arrowheads).

Discussion

γ-tubulin disperses on MT bundles in Mic during elongation of meiotic crescent

By observing the distribution of γ-tubulin during the crescent phase, a dynamic change of arrangement of MT minus ends in the crescent MT bundles was revealed. At the beginning of crescent elongation, γ-tubulin was localized at one end of the crescent (Fig. 10b, arrowhead), and MT bundles polymerized from this area (Fig. 10b, arrow). During elongation of the crescent, this strong aggregation of γ-tubulin was cancelled over time (Fig. 10c, arrowhead), and finally γ-tubulin dispersed all over the MT bundles in the fully elongated crescent (Fig. 10d). This change of the distribution of γ-tubulin during the crescent elongation can be explained by two hypotheses; 1) mutual sliding of crescent MTs or 2) *de novo* polymerization of MTs from γ-tubulin released from the end of the crescent. Since γ-tubulin distributed uniformly on MT bundles of the fully elongated crescent, the polarity of MTs consisting the crescent was not clear. The polarity can be one-directional or random.

Bipolarity of meiotic spindle is established during shortening of crescent

Corresponding to the condensation of Mic chromosome (Fig. 10e, asterisk), an elongated crescent started to be shortened. MTs were quickly bundled at the chromosome-free region in the crescent (Fig. 10e, arrow), which suggests the existence of MT bundling protein in Mic. During shortening of the crescent, γ-tubulin gradually accumulated at both ends of crescent MT bundles (Fig. 10e, f, f', arrowheads). The accumulation was clearer when the length of the crescent became closer to the length of the meiotic spindle (Fig. 11a, arrowheads). Mechanism of shortening of the crescent can be hypothesized in two ways; 1) depolymerization and re-polymerization of MT bundles or 2) mutual sliding of MTs in the MT bundles. In the second hypothesis, gathering of MT minus ends can be explained by the activity of MT minus end crosslinkers like cytoplasmic dynein and kinesin-14 family protein. As described in

31

chapter 1 of this thesis, a part of γ-tubulin in MT bundles was assorted into the ends of MT bundle to form spindle poles (Fig. 2c, arrowheads) in Mic mitosis during vegetative growth. Similar MT sliding mechanism is likely to regulate meiotic spindle formation as well. In any case, the accumulation pattern of γ-tubulin during the crescent shortening demonstrates that the bipolarity of *Tetrahymena* meiotic spindle is established during shortening of the meiotic crescent.

γ-tubulin accumulates on the selected gametic nucleus

Here, I demonstrated that the selected meiotic product was distinguished from the other three products by the specific accumulation of γ-tubulin (Fig. 12B, large arrowheads). Because astral MTs were specifically formed from this selected nucleus (Fig. 12B, arrows), I consider it likely that γ-tubulin aggregates on the outer surface of the selected nuclear envelope and induces polymerization of cytoplasmic MTs. Since γ-tubulin preferentially accumulated on the conjugation junction during nuclear selection (Fig. 12B, small arrowhead), I consider that γ-tubulin initially accumulate on the conjugation junction, and then, some γ-tubulin spread to the surface of the first-comer meiotic product when it touches the conjugation junction. Moreover, the accumulation of γ-tubulin on the selected gametic nucleus persisted during later stages, such as gametogenic mitosis, pronuclear migration, pronuclear exchange, fertilization, and post-zygotic division. This finding suggests that an unknown mechanism maintains γ-tubulin on the selected gametic nucleus, distinguishing it from other, unselected meiotic products. Thus γ-tubulin accumulating on the selected nucleus may play an essential role in the MT polymerization required for successful conjugation.

Possible mechanisms of nuclear fate determination after meiosis

The *Tetrahymena* citrate synthase, which forms a 14-nm filament in vitro (Numata et al., 1980, 1991; Takeda et al., 1997), shows preferential accumulation on the selected meiotic product (Numata et al., 1985; Takagi et al., 1991), similar to MTs. The filaments of citrate synthase are formed from the conjugation junction just before nuclear selection, and later, the citrate synthase accumulates on selected meiotic product (Numata et al., 1985; Takagi et al., 1991). The distribution of γ-tubulin and the citrate synthase suggests that the aggregation of γ-tubulin on the conjugation junction may facilitate the filament formation of the citrate synthase. Numerous filaments of the citrate synthase originated from the conjugation junction (Takagi et al., 1991) may help the recruitment of meiotic product to the conjugation junction. Furthermore, the gene coding this citrate synthase (*CIT1*) is up-regulated during the post-meiotic phase according to TetraFGD (Xiong et al., 2013). This citrate synthase might be involved in the determination of nuclear fate by promoting the citric acid (TCA) cycle in peripheral mitochondria, thereby inhibiting activation of the apoptotic pathway. Indeed, a recent study showed that the treatment of nicotinamide adenine dinucleotide (NAD^+), a major material of TCA cycle, decreases the chance of apoptosis in rat cells (Hong et al., 2013). *Tetrehymana* Genome Database (TGD; http://ciliate.org/) (Stover et al., 2006, 2012) contains eight putative citrate synthase genes, and three of them are up-regulated during nuclear selection according to TetraFGD (Xiong et al., 2013). Knockout experiment of these three citrate synthase genes is necessary to demonstrate the involvement of citrate synthases in nuclear fate determination.

Possible roles of astral MTs in posterior-to-anterior migration and nuclear fusion

My finding that the mitotic spindle during gametogenic mitosis was thick, with a bright fluorescent signal for α-tubulin (Fig. 12D, arrow), suggests that many free tubulin dimers in the cytoplasm participated in the construction of the spindle MTs. Because all nuclear division

of *Tetrahymena* proceeds without nuclear envelope breakdown ("closed" nuclear division), I consider that these tubulin dimers must be transported into the Mic through its nuclear pores. After gametogenic mitosis is completed, the concentration of free tubulin dimers would be expected to increase around the pronuclei because of depolymerization of the spindle MTs, and these free tubulin dimers could then be re-polymerized into cytoplasmic MTs. This is a possible explanation for the sudden polymerization of astral MTs from the surface of daughter pronuclei on the completion of gametogenic mitosis (Fig. 12E, H, arrows). The astral MTs polymerized from the posterior pronucleus stretched toward the destination of the pronucleus during posterior-to-anterior migration (Fig. 12E, arrow). Similar astral MTs were formed from the basket surrounding the anterior pronucleus (Fig. 12H, arrow). The results suggest that the interaction between the astral MTs of the two pronuclei is important for posterior-to-anterior migration. Furthermore, because γ-tubulin and the associated MTs (Fig. 12F, small arrowheads) were distributed on the whole surface of the pronuclei after pronuclear exchange was completed, it is reasonable to speculate that astral MTs surrounding the pronuclei participated in pronuclear fusion.

In animal cells, after fertilization, both female and male pronuclei approach the sperm centrosome by MT-motor-directed movement along centrosomal astral MTs (Gönczy et al., 1999). Detailed studies of *Caenorhabditis elegans* have demonstrated that the attachment and minus-end-directed movement of nuclei requires the function of a pair of membrane proteins, SUN-1 and ZYG-12 (Malone et al., 2003; Minn et al., 2009), which connect nuclei to the cytoplasmic dynein complex (an MT minus-end motor). Pronuclear fusion during vertebrate fertilization seems to be driven by a similar mechanism, in that the protein domain structure and cellular function of zebrafish Lrmp (Lindeman and Pelegri, 2012) corresponds to that of *C. elegans* ZYG-12, although the sequence similarity between the vertebrate and invertebrate proteins is not statistically significant. Because the astral MTs were produced from pronuclei

(Fig. 12E, H, arrows), the migration of pronuclei and subsequent pronuclear fusion in *Tetrahymena* can be more simply explained by the involvement of MT-crosslinking minus-end motors, which can shorten the mutual distance between the MT minus-ends on the surfaces of pronuclei. To reveal the function of pronuclei-directed astral MTs, an analysis of MT-associated proteins, including cytoplasmic dynein and kinesin-14 (another MT minus-end motor), is required.

I observed that nucleus-associated γ-tubulin persisted after fertilization (Fig. 12G, arrowhead). Both daughter nuclei of the first post-zygotic division were labeled with γ-tubulin (Fig. 13B, arrowheads). Because the two daughter nuclei come close to each other after the first post-zygotic division (Fig. 13C, arrowheads; Cole and Sugai, 2012), accumulation of γ-tubulin may be required for movement of these daughter nuclei as well as the earlier pronuclear migration. The amount of cytoplasmic MTs around these daughter nuclei (Fig. 13C, small arrowheads) appeared less than that around the pronuclei (Fig. 12E, H, arrows), probably because the depolymerization of spindle MTs after the first post-zygotic division is delayed (Fig. 13C, arrow) compared with that after gametogenic mitosis (Fig. 12E, 2nd left panel). At anaphase of the second post-zygotic division, the γ-tubulin signal was reduced compared with that at the first post-zygotic division (Fig. 13D, arrowheads), suggesting that accumulation of γ-tubulin was no longer required by the start of the second post-zygotic division.

Possible function of abundant cytoplasmic MTs formed after post-zygotic divisions

I observed that the network of cytoplasmic MTs was highly augmented when the MT spindle of the second post-zygotic division disappeared (Fig. 13E, 2nd left panel), probably because of accelerated MT polymerization with the increased concentration of free tubulin dimers. These cytoplasmic MTs seem to originate throughout the cell cortex rather than just from the surfaces of nuclei (Fig. 13E, 2nd left panel).

By the end of the second post-zygotic division, two new Macs and two new Mics are differentiated. These move to characteristic positions relative to each other and the parental Mac: the two Mics are positioned between the two new Macs, and the parental Mac is positioned at the far posterior end of the cell (Cole and Sugai, 2012; Fig. 13G, left panel). This change of arrangement of the new Macs and Mics and the parental Mac is more complex than the one-directional posterior-to-anterior migration of the pronucleus, because it includes multiple nuclear movements in different directions happening at the same time and place. I hypothesize that each nucleus is attracted by a specific signal that comes from a specific position of the cell cortex, and that this signal is mediated by the network of cytoplasmic MTs. To reveal the mechanism behind such nuclear movements, an analysis of the MT-associated proteins is required.

Presence of γ-tubulin in swelling new Mics

During the polymerization of abundant cytoplasmic MTs that occurs after second post-zygotic divisions, γ-tubulin enters the parental Mac (Fig. 13E, arrow), and scattered MTs formed in the parental Mac (Fig. 13E, small arrowhead). This distribution of γ-tubulin coincides with the previously reported localization of Mic-derived small RNAs, which are required for new Mac development, as outlined below. During conjugation, 28- to 30-nucleotide small RNAs (scan RNAs; scnRNAs) are transcribed from intact Mic chromosomes and enter the parental Mac, and the scnRNAs corresponding to parental Mac DNA including gene-coding regions will be degraded in the parental Mac. The remaining internal-elimination-sequence- specific (IES-specific) scnRNAs are transferred into the new Macs, resulting in the deletion of IESs and fragmentation of the new Mac chromosomes (Karrer, 2000, 2012; Schoeberl et al., 2012). The change of distribution of γ-tubulin observed here resembles the pattern of translocation of scnRNAs from parental Mac to new Macs. With

36

the condensation of the parental Mac, γ-tubulin and scattered MTs in the parental Mac quickly disappeared (Fig. 13F, arrow), and instead, some γ-tubulin molecules entered the swelling new Macs (Fig. 13F, G, large arrowheads). Compared with the scattered MTs in the parental Mac (Fig. 13E, small arrowhead), the MTs in the new Macs were less abundant (Fig. 13H, arrowheads), suggesting that transportation of tubulin dimers into the new Macs was very limited. Plus, some γ-tubulin in the new Macs did not colocalize with MTs (Fig. 13H, arrows). The coupled translocation pattern of γ-tubulin and scnRNA leads me to speculate that γ-tubulin binds to some of the scnRNA in the parental Mac and that together they are actively or passively transported into the new Macs. Further biochemical experiments are required to explore this possibility. Because γ-tubulin enters the dividing Mac only during vegetative growth (Chapter 1, Fig. 6; Joachimiak et al., 2007), the γ-tubulin in parental and new Macs probably has an unknown conjugation-specific function.

I demonstrated here that the determination of gametic nuclear fate is achieved by the accumulation of γ-tubulin on a meiotic product. The accumulation of γ-tubulin enables the pronuclei to produce astral MTs after gametogenic mitosis. I propose that mutual attraction of astral MTs originating from the pronuclei plays an essential role in formation of the zygotic nucleus in *Tetrahymena*. This study clearly highlights the involvement of cytoskeletal regulation in the modulation of germline nuclear behavior during ciliate reproduction.

Conclusions

    I demonstrated that the bipolarity of meiotic spindle is established during shortening of the prophase crescent. The 'Selected' meiotic product is distinguished from non-selected products by strong accumulation of γ-tubulin. Astral MTs polymerized from the surface of pronuclei seem to be important for pronuclear migration and fertilization. Moreover, γ-tubulin may be involved in development of new Macs.

Analysis of the localization and the function of *Tetrahymena* kinesin-14 during mitosis, amitosis and meiosis

Abstract

To reveal the molecular mechanism that regulates the dynamics of MT minus ends during three types of nuclear division (mitosis, meiosis and amitosis), I performed gene knockout (KO) of kinesin-14 genes, which is known as MT-minus end motor in animal cell, in the ciliate *Tetrahymena*. I identified two homologs (named *KIN14A* and *KIN14B*) of human and yeast mitotic kinesin-14s in the *Tetrahymena* genome. The chromosome segregation during mitosis and meiosis is severely disturbed in *KIN14A*-KO cell. The defective meiotic spindle formation suggested that KIN14A is involved in the formation of meiotic spindle poles by promoting MT sliding. Indeed, EGFP-tagged recombinant KIN14A preferentially accumulated at the spindle poles during the shortening of the meiotic crescent. In contrast, double KO of *KIN14A* and *14B* did not affect amitosis during vegetative growth. This study showed the differentiation of MT regulation mechanism of amitosis, the ciliate-specific Mac division, from mitosis and meiosis.

Introduction

In mitosis of animal cells, astral MTs polymerized from duplicated MTOCs, namely centrosomes, are cross-linked and take anti-parallel configuration following nuclear envelope break down (NEBD). Kinesin-5 family protein, Eg5 is plus-end-directed MT motor essential for formation of the anti-parallel MT structure (Tao et al., 2006). The motor domain is located in the N-terminal portion of the primary structure of Eg5, which migrates to the MT plus-end in an ATP-dependent manner. Eg5 forms tetramer via its C-terminal coiled-coil domain, thus Eg5 is able to cross-link MT plus-ends (Cole et al., 1994). Accordingly, two duplicated centrosomes are faced each other separated by the bundled MTs, which is the fundamental structure of bipolar spindles (reviewed in Valentine et al., 2006). By contrast, MT minus-end motors are important for stabilization of spindle pole structures (Tao et al., 2006). Cytoplasmic dynein is a large complex of various protein subunits including heavy chain and many regulatory light chains. Cytoplasmic dynein crosslinks MT by the MT attachment of its 'head' and 'tail', and is motile to the MT minus-end in an ATP-dependent manner (Wu et al., 2006; Akhmanova and Hammer, 2010; Tanenbaum and Medema, 2010). While most of kinesin family proteins behave as plus-end-directed motors, kinesin-14 (Ncd) subfamily protein has the activity to move toward the minus-end of MTs (Sharp et al., 1999). Kinesin-14 is identified as an MT motor which is essential for mitosis and meiosis in *Drosophila* (Endow et al., 1990). Kinesin-14 is also called as "C-kinesin" because its ATP-dependent motor domain is positioned in the C-terminal domain (Chandra et al., 1993). Kinesin-14 forms dimer via coiled-coil domain of the N-terminal domain. The N-terminal MT-binding domain composed by 18 amino acids binds an MT in ATP-independent manner (Karabay and Walker, 1999, 2003). Therefore, the dimer of Kinesin-14 behaves as an MT-crosslinking motor. Although kinesin-14 is widely conserved as a mitotic motor among many eukaryotes, the amino acid sequences of the N-terminal region are varied between species. The 18-amino-acid

40

MT-binding domain identified in *Drosophila* Kinesin-14 is not conserved in other eukaryotes. For example, mouse kinesin-14 forms tetramer by its coiled-coil domain just like Eg5, and crosslink MT minus-ends (Schuh and Ellenberg, 2007). There are some diverse kinesin-14 proteins which work as minus-end-directed transporter like human KIF25 (Groth-Pedersen et al., 2012).

MT minus-end-directed motors cause an accumulation of minus-ends (minus-end-focusing) as a result of their activity of cross-linking MTs, which is essential for formation of spindle poles during mitosis and meiosis (Hatsumi and Endow, 1992; Burbank et al., 2007). Eg5 and minus-end motors behave antagonistically to stabilize spindle structure (Tao et al., 2006). Chromosomes are anchored to spindle poles through integration of kinetochore MT (k-fiber) minus ends to poles. In closed mitosis of yeast, spindle pole body (SPB) which is embedded in nuclear envelope serves as MTOC, and a similar MT-motor-dependent mechanism govern the spindle function (reviewed in Winey and Bloom, 2012).

I studied the distribution of γ-tubulin which works as MTOC during Mic mitosis and Mac amitosis of *Tetrahymena* to reveal the mechanism of mitotic spindle formation in ciliate. During interphase, several dotted signals of γ-tubulin were detected on the surface of Mic. In mitotic phase, intranuclear MTs were suddenly formed. Most of those MTs formed a bundle, and γ-tubulin was distributed along these MT bundles. As *Tetrahymena* does not have congregative MTOC like centrosome or SPB, astral MTs were not observed in Mic mitosis (Chapter 1, Fig. 2b). MT bundles formed at the beginning of mitosis were persistent during whole mitosis. Thus, these MT bundles are likely to fulfill functions equivalent to 'inter-polar MT' of animal cells. Since the signal of γ-tubulin at the both ends of inter-polar MT bundle became clear by the anaphase A, spindle poles of *Tetrahymena* mitosis seems to be organized as the result of an assortment of γ-tubulin to distal ends of MTs. MT minus-end motors are

possibly involved in accumulation of γ-tubulin during mitosis. In contrast, amitosis of Mac did not show bipolar arrangement of γ-tubulin. Instead, γ-tubulin dots were dispersed in the whole dividing Mac and polymerize randomly oriented MTs in Mac. Importantly, γ-tubulin dots were temporary accumulated at the center of Mac just before the initiation of Mac elongation. Therefore, as in Mic mitosis, MT minus-end motors may be involved in MT regulation during amitosis.

Both of ciliates, *Tetrahymena* and *Paramecium* lack homolog of kinesin-5 (Eg5) motor (Wickstead et al, 2010), and alternative MT plus-end motors have not reported. On the other hand, gene KO of *Tetrahymena* cytoplasmic dynein (*DYH1*, *DYH2*) revealed the essential role of DYH1 in chromosome segregation during Mic mitosis (Lee et al., 1999). DYH2 is required for pattern formation of cortical MTs, but not for nuclear segregation.

In this chapter, I will show the results of gene KO experiments of *Tetrahymena* kinesin-14 (*Ncd*) subfamily genes (*KIN14A, KIN14B*), whose functions have been unknown. The mechanism of mitosis and amitosis will be discussed in terms of requirement of the activity of MT minus-end motors during mitosis and amitosis.

Materials and Methods

Gene KO experiment

All procedures were performed as previously described by Dave et al (2009). Strains B2086 and CU428 were used for germline transformation. Genotypes of KO strains were confirmed by PCR (Fig. 16).

EGFP-tagging experiment

All procedures were performed as previously described by Shang et al (2002b). Strain CU522 was used for transformation.

Indirect immunofluorescence

Cells were fixed using the methods described in Chapter 1. Fixed cells were treated with mouse anti-chicken α-tubulin antibody (Calbiochem, Darmstadt, Germany; 1/300 dil.) and rabbit anti-GFP antibody (1/300 dil.) at room temperature, overnight. After washing, cells were incubated with FITC-conjugated goat anti-mouse IgG antiserum (TAGO, Burlingame, CA; 1/300 dil.) and Rhodamine-conjugated goat anti-rabbit IgG antiserum (Kirkegaard & Perry Laboratories, Gaithersburg, MD; 1/300 dil.) for 6 h. DNA was stained with DAPI (final conc. 1 μg/mL). Cells were observed under a confocal laser scanning microscope (Carl Zeiss, Oberkochen, Germany, LSM700 with an alpha Plan-Apochromat 100× lens, N.A. 1.46).

Phylogenetic analysis

Tetrahymena kinesin protein sequences were searched from Mac genome database (TGD: http://ciliate.org/index.php/home/welcome), and their motor domains were identified by NCBI Protein BLAST (http://blast.ncbi.nlm.nih.gov/) or SMART program (http://smart.embl-

43

heidelberg.de/). Protein multiple alignment was carried out by free sequence analysis software 'BioEdit' (version 7.0.5.3; http://www.mbio.ncsu.edu/bioedit/bioedit.html), and a sequence from the 3rd to the 8th beta sheet of the motor domain, including phosphate binding site for ATP ($<$235 a.a.) (Kull *et al*., 1996; Sablin *et al*., 1996), was extracted and imperfectly aligned gaps were excluded manually. Sequence of human and yeast kinesin proteins were extracted by the same procedures. Phylogenetic tree was drawn for these extracted protein sequences by Clustal W program version 1.83 (http://clustalw.ddbj.nig.ac.jp/). Bootstrap proportions (%) were obtained from 1000 pseudoreplicate datasets. Although the similarity of each kinesin subfamily of human and yeast vary between subfamilies, each subfamily has at least 30% similarity (YK, unpublished data). Therefore, *Tetrahymena* kinesins showing >30% identity to human or yeast kinesin were considered to be their orthologues while *Tetrahymena* kinesins showing <30% identity were considered to be species-specific kinesins. Coiled-coil region was predicted by SMART server and COILS server (http://www.ch.embnet.org/software/COILS_ form.html).

Results and Discussion

Two homologs of *Ncd* exist on *Tetrahymena* genome

By searching *Tetrahymena* genome database (TGD), I identified four kinesin genes which have a motor domain in their C-terminal domain (C-kinesin). I performed a phylogenetic analysis for amino acid sequences of 82 *Tetrahymena* kinesin genes and kinesin genes of human, fission yeast and budding yeast. The result showed that two out of the four *Tetrahymena* C-kinesins were homologs of mitotic minus-end kinesin (*Ncd*) as they clustered together with other Ncd homologs of human (*KIFC1*), fission yeast (*Klp1*) and budding yeast (*KAR3*) (Fig. 14, 'Kinesin-14A'). I named these two putative mitotic C-kinesins of *Tetrahymena* as *KIN14A* and *KIN14B* for further genetic analysis. The remaining two C-kinesins of *Tetrahymena* were reported to belong to "kinesin-14D" cluster in the exhaustive phylogenic study of Wickstead et al (2010), although I was unable to detect their homology with the members of "kinesin-14D" subfamily (Fig. 15, orange squares). In this report (2010), *KIN14A* and *KIN14B* were clustered in "kinesin-14A" together with *Ncd* homologs. Kinesin-14D cluster proposed in this report is relatively diverse when compared to the mitotic kinesin-14A cluster, and contains various kinesins of different functions. For example, kinesin-14D contains human transporter kinesin KIF25 (Groth-Pedersen et al., 2012), and plus-end crosslinker kinesin which forms anti-parallel phragmoplast MTs during plant cell division (Hiwatashi et al., 2008).

In this study, I performed gene KOs of *KIN14A* and *KIN14B*, because these two kinesins are expected to function as MT minus-end motor in *Tetrahymena*.

KIN14A-KO caused an insufficiency of mitotic chromosome segregation

Single gene KOs of *KIN14A* and *KIN14B* were performed (Fig. 16). As a result, the segregation of Mic was severely disturbed in *KIN14A*-KO cells, but not in *KIN14B*-KO cells

45

(Table IV). About 80% of *KIN14A*-KO cells showed abnormal chromosome segregation during mitosis (Table IV, Fig. 17, arrowheads). Co-staining of MT and DNA showed that *KIN14A*-KO cell could form MT bundles during mitosis, but Mic chromosomes were usually left in the middle of those spindle MTs during anaphase (Fig. 18, arrowheads). Inefficiency of chromosome segregation in *KIN14A*-KO cells can be explained by the failure of MT-minus-end-motor-directed anchoring of kinetochore MTs to spindle poles. Presumably, KIN14A can crosslink MTs and stabilize the minus-ends of kinetochore MTs at the spindle poles.

Because bundles of MTs were formed without the expression of *KIN14A* (Fig. 18, arrow), unknown MT crosslinker is likely to be involved in mitosis. Normal segregation of Mic chromosome in *KIN14A*-KO cell (less than 20%, Table IV) may be the result of coincidental stabilization of kinetochore MT near the spindle poles.

During amitosis, abundant polymerization and dynamic reorganization of intra-Mac MTs were involved in the longitudinal elongation of Mac (see Chapter 1, Fig. 1). Just before the beginning of Mac elongation, γ-tubulin accumulated at the center of Mac and at the same time, polymerization of MTs was enhanced there (Chapter 1, Fig. 6, stage 2). Single gene KO of neither *KIN14A* nor *KIN14B* influenced the normal amitosis. Double gene KO of *KIN14A & 14B* showed mitotic defect quite similar with *KIN14A* single KO, while amitosis was normal (data not shown). In addition, MT organization in Mac seemed normal in *KIN14A*-KO cells (Fig. 18), and transient accumulation of MTs at the center of Mac was also observed (data not shown). Therefore, mitotic KIN14A, which is involved in proper Mic segregation, is not required for organization of MTs in amitosis. However, the multiple gene KO for all of the four C-kinesins including *KIN14A & 14B* and kinesin-14D genes and cytoplasmic dynein *DYH1* is necessary to completely eliminate the possibility of involvement of MT minus-end motors in Mac amitosis.

KIN14A is localized on spindle MTs during mitosis

Next, I analyzed the cellular localization of KIN14A by expressing recombinant protein, EGFP-KIN14A, under the control of a cadmium-ion-inducible promoter (*MTT1* promoter) in *Tetrahymena* cells. Since the fluorescence signal of EGFP in living cells during vegetative growth was too weak to detect (data not shown), the cell was triple-stained with anti-GFP and anti-α-tubulin antibodies and DAPI and observed. The confocal microscopy of the triple-stained cell clearly showed that KIN14A was localized along the whole Mic spindle MTs during mitosis (Fig. 19, arrowhead). In animal cells, mitotic kinesin-14 preferentially accumulates at spindle poles. The distribution pattern of KIN14A as well as γ-tubulin suggests that many MT minus-ends are left in the middle of the mitotic spindle in *Tetrahymena* (see Chapter 1, Fig. 2c, d). Presumably, unknown MT-bundling protein can produce an alternative form of inter-polar MT bundles in which not all of the MT-minus ends are positioned at the spindle poles. Since KIN14A is essential for proper chromosome segregation, the role of KIN14A during mitosis may be an anchoring of kinetochore MTs to both spindle poles.

KIN14A is essential for chromosome segregation in meiosis

The bipolarity of meiotic spindle is established during the shortening of the crescent, as judged by the distribution of γ-tubulin (Chapter 2, Fig. 10). The phenotype of *KIN14A*-KO cells during meiosis was analyzed by immunofluorescence. Double-staining image of MTs and DNA showed that the shortening of MTs in the crescent was not accomplished in *KIN14A*-KO cells (Fig. 21d, arrowheads). This phenotype demonstrated that KIN14A is essential for the formation of proper meiotic spindle probably by the MT-sliding mediated compaction of MTs. Meiotic spindle seemed to be highly dependent on KIN14A compared to mitotic spindle. This is probably because the bipolar spindle formation required the compaction of long crescent

MTs in meiosis I. MT sliding caused by KIN14A is likely to gather MT minus-ends and to cause crescent shortening at the same time.

The condensed chromosomes in disrupted meiotic spindle of *KIN14A*-KO pair cells were dispersed, and eventually, *KIN14A*-KO cells caused an irregular (most likely random) chromosome partition during meiosis (Fig. 21e, arrowheads). The movement of chromosomes between MT bundles in *KIN14A*-KO cells was highly erratic because sometimes all chromosomes were left at one end of the MT bundle and not partitioned at all (Fig. 21e, left cell). Nuclear 'selection' following meiosis was often observed, but neither the size nor the number of meiotic products was normal (Fig 21g, arrowheads). Therefore, *KIN14A*-dependent proper segregation of chromosomes during meiosis is essential for conjugation.

To analyze the localization of KIN14A during conjugation, EGFP-KIN14A-overexpressing strain and wildtype strain were crossed and observed. The fluorescent signals of EGFP-KIN14A gradually accumulated on the edges of Mic during crescent shortening (Fig. 22a, arrowheads). Unlike vegetative phase, the fluorescent signal in Mic of living cell during conjugation is enough for detection. Triple-staining with anti-GFP and anti-α-tubulin antibodies and DAPI of the pair of cells demonstrated the accumulation of KIN14A to both ends of the meiotic spindle MTs (Fig. 22e, arrowheads). Since the localization of KIN14A is very similar to that of γ-tubulin during meiotic spindle formation (Chapter 2, Fig. 11b, arrowheads), KIN14A is most likely to accumulate on MT minus-ends and participate in the formation of meiotic spindle poles by its minus-end-directed motility (Fig. 23).

Conclusions

In this chapter, I demonstrate that *Tetrahymena* kinesin-14, KIN14A, is required for proper chromosome segregation during mitosis of vegetative growth. Probably, unknown MT-bundling protein can substitute for the mitotic function of KIN14A because about 10% of mitotic spindle of *KIN14A*-KO cells can apparently segregate Mic chromosomes equally. On the other hand, KIN14A is essential for meiotic spindle formation during conjugation. KIN14A accumulates on MT minus-ends during crescent shortening, and forms spindle poles by focusing MT minus-ends. This function of KIN14A during dynamic meiotic spindle formation is indispensable and cannot be substituted for by any other MT-associated proteins. Since Mac amitosis does not require both of KIN14A and 14B, the accumulation of γ-tubulin and MTs during amitosis is most likely minus-end motor independent. This study clearly showed the differences of molecular mechanism between mitosis, amitosis and meiosis in ciliate.

General Discussion

This study is focused on the difference of molecular mechanisms of ciliate mitosis, meiosis and amitosis. By analyzing the localization of γ-tubulin, I showed that the MT formation during mitosis and amitosis was quite different; mitosis with a bipolar spindle and amitosis with randomly-directed MT formation and following assortment of γ-tubulin. Though mitosis required MT minus-end motor KIN14A, both of mitotic kinesin-14 homologs (KIN14A & 14B) were not required for amitotic MT regulation. Since KIN14A was essential for chromosome segregation during mitosis, it is likely that KIN14A is important in stabilizing the minus-ends of kinetochore MTs. In other words, amitosis does not require KIN14A because kinetochore MTs do not participate in amitosis. Importantly, the segregation of bivalent chromosomes during meiosis was severely disturbed by gene KO of KIN14A. It seems that the segregation of dense and larger chromosomes in meiosis is highly dependent on the MT minus-end motor because it requires more power to pull such large chromosomes. This study succeeded to capture the difference of mechanisms of mitosis, meiosis and amitosis, and provides a scaffold for further detailed genetic and biochemical studies.

.

Acknowledgements

References

Akematsu T, Fukuda Y, Attiq R, Pearlman RE (2014) Role of class III phosphatidylinositol 3-kinase during programmed nuclear death of *Tetrahymena thermophila*. Autophagy 10: 1-17, in press

Akematsu T, Pearlman RE, Endoh H (2010) Gigantic macroautophagy in programmed nuclear death of *Tetrahymena thermophila*. Autophagy 6: 901-911

Akhmanova A, Hammer JA 3rd (2010) Linking molecular motors to membrane cargo. Curr Opin Cell Biol 22:479-487

Allen S, Gibson I (1972) Genome amplification and gene expression in the ciliate macronucleus. Biochem Genet 6:293-313

Bouissou A, Verollet C, Sousa A, Sampaio P, Wright M, Sunkel CE, Merdes A, Raynaud-Messina B (2009) γ-tubulin ring complexes regulate microtubule plus end dynamics. J Cell Biol 187:327-334

Burbank KS, Mitchison TJ, Fisher DS (2007) Slide-and-cluster models for spindle assembly. Curr Biol 17 : 1373-1383

Chandra R, Salmon ED, Erickson HP, Lockhart A, Endow SA (1993) Structural and functional domains of the Drosophila ncd microtubule motor protein. J Biol Chem 268: 9005-9013

Cole DG, Saxton WM, Sheehan KB, Scholey JM (1994) A "slow" homotetrameric kinesin-related motor protein purified from *Drosophila* embryos. J Biol Chem 269: 22913-22916

Cole E (2006) The *Tetrahymena* conjugation junction. In "Cell-Cell Channels" Ed by Baluska F, Volkmann D, Barlow PW, Springer, New York, pp 39-62

Cole E, Sugai T (2012) Developmental progression of *Tetrahymena* through the cell cycle and conjugation. In "Methods in Cell Biology, Volume 109, *Tetrahymena thermophila*" Ed by Collins K, Academic Press, San Diego, pp 177–236

Dave D, Wloga D, Gaertig J (2009) Manipulating ciliary protein-encoding genes in *Tetrahymena thermophila*. Methods Cell Biol vol. 93: 1-20

Davidsona L, LaFountain JR Jr. (1975) Mitosis and early meiosis in *Tetrahymena pyriformis* and the evolution of mitosis in the phylum ciliophora. Biosystems 7:326-336

Ding DQ, Chikashige Y, Haraguchi T, Hiraoka Y (1998) Oscillatory nuclear movement in fission yeast meiotic prophase is driven by astral microtubules, as revealed by continuous observation of chromosomes and microtubules in living cells. J Cell Sci 111: 701-712

Endow SA, Henikoff S, Soler-Niedziela L (1990) Mediation of meiotic and early mitotic chromosome segregation in *Drosophila* by a protein related to kinesin. Nature 345: 81-83

Falk H, Wunderlich F, Franke WW (1968) Microtubular structures in macronuclei of synchronously dividing *Tetrahymena pyriformis*. J. Protozool 15:776-780

Fujiu K, Numata O (2000) Reorganization of microtubules in the amitotically dividing macronucleus of *Tetrahymena*. Cell Motil Cytoskel 46:17-27

Gaertig J, Fleury A (1992) Spatio-temporal reorganization of intracytoplasmic microtubules is associated with nuclear selection and differentiation during the developmental process in the ciliate *Tetrahymena thermophila*. Protoplasma 197:74-87

Gönczy P, Pichler S, Kirkham M, Hyman AA (1999) Cytoplasmic dynein is required for distinct aspects of MTOC positioning, including centrosome separation, in the one cell stage *Caenorhabditis elegans* embryo. J Cell Biol 147: 135-150

Goshima G, Mayer M, Zhang N, Stuurman N, Vale RD (2008) Augmin: a protein complex required for centrosome-independent microtubule generation within the spindle. J Cell Biol 181:421-429

Groth-Pedersen L, Aits S, Corcelle-Termeau E, Petersen NH, Nylandsted J, Jäättelä M (2012) Identification of cytoskeleton-associated proteins essential for lysosomal stability and survival of human cancer cells. PLoS One 7: e45381

Hamilton EP, Suhr-Jessen PB, Orias E (1988) Pronuclear fusion failure: an alternate conjugational pathway in *Tetrahymena thermophila*, induced by vinblastine. Genetics 118: 627-636

Haren L, Remy MH, Bazin I, Callebaut I, Wright M, Merdes A (2006) NEDD1-dependent recruitment of the γ-tubulin ring complex to the centrosome is necessary for centriole duplication and spindle assembly. J Cell Biol 172: 505-515

Hatsumi M, Endow SA (1992) The Drosophila ncd microtubule motor protein is spindle-associated in meiotic and mitotic cells. J Cell Sci 103: 1013-1020

Hiwatashi Y, Obara M, Sato Y, Fujita T, Murata T, Hasebe M (2008) Kinesins are indispensable for interdigitation of phragmoplast microtubules in the moss *Physcomitrella patens*. Plant Cell 20: 3094-3106

Hong Y, Nie H, Wu D, Wei X, Ding X, Ying W (2013) NAD^+ treatment prevents rotenone-induced apoptosis and necrosis of differentiated PC12 cells. Neurosci Lett, in press

Ito J, Lee YC, Scherbaum OH (1968) Intranuclear microtubules in *Tetrahymena pyriformis* GL. Exp Cell Res 53:85-93

Joachimiak E, Pucciarelli S, Barchetta S, Ballarini P, Kaczanowska J, Miceli C (2007) Cell cycle-dependent expression of γ-tubulin in the amicronuclear ciliate *Tetrahymena pyriformis*. Protist 158:39-50

Kaczanowski A, Gaertig J, Kubiak J (1985) Effect of the antitubulin drug nocodazole on meiosis and post-meiotic development in *Tetrahymena thermophila*. Exp Cell Res 158: 244-256

Kaczanowski A, Ramel M, Kaczanowska J, Wheatley D (1991) Differentiation in conjugating pairs of *Tetrahymena* treated with the antitubulin drug nocodazole. Exp Cell Res 195: 330-337

Karabay A, Walker RA (1999) Identification of microtubule binding sites in the Ncd tail domain. Biochemistry 38: 1838-1849

Karabay A, Walker RA (2003) Identification of Ncd tail domain-binding sites on the tubulin dimer. Biochem Biophys Res Commun 305: 523-528

Karrer KM (2000) *Tetrahymena* genetics: two nuclei are better than one. In "Methods in Cell Biology, Volume 62, *Tetrahymena thermophila*" Ed by Asai DJ, Forney JD, Academic Press, San Diego, pp 127-186

Karrer KM (2012) Nuclear dualism. In "Methods in Cell Biology, Volume 109, *Tetrahymena thermophila*" Ed by Collins K, Academic Press, San Diego, pp 29-52

Kollman JM, Polka JK, Zelter A, Davis TN, Agard DA (2010) Microtubule nucleating γ-TuSC assembles structures with 13-fold microtubule-like symmetry. Nature 466:879-882

Kull FJ, Sablin EP, Lau R, Fletterick RJ, Vale RD (1996) Crystal structure of the kinesin motor domain reveals a structural similarity to myosin. Nature 380:550-555

Lee S, Wisniewski JC, Dentler WL, Asai DJ (1999) Gene knockouts reveal separate functions for two cytoplasmic dyneins in *Tetrahymena thermophila*. Mol Biol Cell 10: 771-784

Lindeman RE, Pelegri F (2012) Localized products of futile cycle/lrmp promote centrosome-nucleus attachment in the zebrafish zygote. Curr Biol 22: 843-851

Loidl J, Lukaszewicz A, Howard-Till RA, Koestler T (2012) The *Tetrahymena* meiotic chromosome bouquet is organized by centromeres and promotes interhomolog recombination. J Cell Sci 125: 5873-5880

Loidl J, Mochizuki K (2009) *Tetrahymena* meiotic nuclear reorganization is induced by a checkpoint kinase-dependent response to DNA damage. Mol Biol Cell 20: 2428-2437

Loidl J, Scherthan H (2004) Organization and pairing of meiotic chromosomes in the ciliate *Tetrahymena thermophila*. J Cell Sci 117: 5791-5801

Malone CJ, Misner L, Le Bot N, Tsai MC, Campbell JM, Ahringer J, et al. (2003) The *C. elegans* Hook protein, ZYG-12, mediates the essential attachment between the centrosome and nucleus. Cell 115: 825-836

Martindale DW, Allis CD, Bruns PJ (1982) Conjugation in *Tetrahymena thermophila*. A temporal analysis of cytological stages. Exp Cell Res 140: 227-236

McKean PG, Vaughan S, Gull K (2001) The extended tubulin superfamily. J Cell Sci 114:2723-2733

Minn IL, Rolls MM, Hanna-Rose W, Malone CJ. (2009) SUN-1 and ZYG-12, mediators of centrosome-nucleus attachment, are a functional SUN/KASH pair in *Caenorhabditis elegans*. Mol Biol Cell 20: 4586-4595

Mochizuki K, Fine NA, Fujisawa T, Gorovsky MA (2002) Analysis of a piwi-related gene implicates small RNAs in genome rearrangement in Tetrahymena. Cell 110:689-699

Mochizuki K, Novatchkova M, Loidl J (2008) DNA double-strand breaks, but not crossovers, are required for the reorganization of meiotic nuclei in *Tetrahymena*. J Cell Sci 121: 2148-2158

Murata T, Sonobe S, Baskin TI, Hyodo S, Hasezawa S, Nagata T, Horio T, Hasebe M (2005) Microtubule-dependent microtubule nucleation based on recruitment of γ-tubulin in higher plants. Nat Cell Biol 7:961-968

Nakagawa T, Fujiu K, Cole ES, Numata O (2008) Involvement of a 25 kDa *Tetrahymena* Ca^{2+}-binding protein in pronuclear exchange. Cell Struct Funct 33:151-162

Numata O, Takemasa T, Takagi I, Hirono M, Hirano H, Chiba J, et al. (1991) *Tetrahymena* 14-nm filament-forming protein has citrate synthase activity. Biochem Biophys Res Commun 174: 1028-1034

Numata O, Sugai T, Watanabe Y (1985) Control of germ cell nuclear behaviour at fertilization by *Tetrahymena* intermediate filament protein. Nature 314: 192-194

Numata O, Yasuda T, Hirabayashi T, Watanabe Y (1980) A new fiber-forming protein from *Tetrahymena pyriformis*. Exp Cell Res 129: 223-230

Oakley CE, Oakley BR (1989) Identification of γ-tubulin, a new member of the tubulin

superfamily encoded by *mipA* gene of *Aspergillus nidulans*. Nature 338:662-664

Orias E, Flacks M (1975) Macronuclear genetics of *Tetrahymena*. I. Random distribution of macronuclear genecopies in *T. pyriformis*, syngen 1. Genetics 79:187-206

Orias JD, Hamilton EP, Orias E (1983) A microtubule meshwork associated with gametic pronucleus transfer across a cell-cell junction. Science 222: 181-183

Piccinni E, Irato P, Coppellotti O, Guidolin L (1987) Biochemical and ultrastructural data on *Tetrahymena pyriformis* treated with copper and cadmium. J Cell Sci 88:283-293

Raikov IB (1982) The protozoan nucleus. Wien, New York: Springer-Verlag. 253 p.

Ray C Jr (1956) Meiosis and nuclear behavior in *Tetrahymena pyriformis*. J Protozool 3: 88–96

Sablin EP, Kull FJ, Cooke R, Vale RD, Fletterick RJ (1996) Crystal structure of the motor domain of the kinesin-related motor ncd. Nature 380:555-559

Schoeberl UE, Kurth HM, Noto T, Mochizuki K (2012) Biased transcription and selective degradation of small RNAs shape the pattern of DNA elimination in *Tetrahymena*. Genes Dev 26: 1729-1742

Schuh M, Ellenberg J (2007) Self-organization of MTOCs replaces centrosome function during acentrosomal spindle assembly in live mouse oocytes. Cell 130: 484-498.

Suganuma Y, Yamamoto H (1992) Conjugation in *Tetrahymena*: Ultrastructure of the meiotic prophase of the micronucleus. Eur J Protistol 28: 434-441

Shang Y, Li B, Gorovsky MA (2002a) *Tetrahymena thermophila* contains a conventional γ-tubulin that is differentially required for the maintenance of different microtubule-organizing centers. J Cell Biol 158: 1195-1206

Shang Y, Song X, Bowen J, Corstanje R, Gao Y, Gaertig J, Gorovsky MA (2002b) A robust inducible-repressible promoter greatly facilitates gene knockouts, conditional expression, and overexpression of homologous and heterologous genes in *Tetrahymena thermophila*. Proc Natl

Acad Sci USA 99: 3734-3739

Sharp DJ, Yu KR, Sisson JC, Sullivan W, Scholey JM (1999) Antagonistic microtubule-sliding motors position mitotic centrosomes in *Drosophila* early embryos. Nat Cell Biol 1: 51-54

Smith JJ, Yakisich JS, Kapler GM, Cole ES, Romero DP (2004) A β-tubulin mutation selectively uncouples nuclear division and cytokinesis in *Tetrahymena thermophila*. Eukary Cell 3:1217-1226

Stover NA, Krieger CJ, Binkley G, Dong Q, Fisk DG, Nash R, et al. (2006) *Tetrahymena* Genome Database (TGD): a new genomic resource for *Tetrahymena thermophila* research. Nucleic Acids Res 34: D500-D503

Stover NA, Punia RS, Bowen MS, Dolins SB, Clark TG (2012) *Tetrahymena* Genome Database Wiki: a community-maintained model organism database. Database 2012: bas007

Stone GE (1968) Synchronized cell division in *Tetrahymena pyriformis* following inhibition with vinblastine. J Cell Biol 39:556-563

Takagi I, Numata O, Watanabe Y (1991) Involvement of 14-nm filament-forming protein and tubulin in gametic pronuclear behavior during conjugation in *Tetrahymena*. J Protozool 38: 345-351

Takeda T, Watanabe Y, Numata O (1997) Direct demonstration of the bifunctional property of *Tetrahymena* 14-nm filament protein/citrate synthase following expression of the gene in *Escherichia coli*. Biochem Biophys Res Commun 237: 205-210

Tamura S, Tsuruhara T, Watanabe Y (1969) Function of nuclear microtubules in macronuclear division of *Tetrahymena pyriformis*. Exp Cell Res 55:351-358

Tanenbaum ME, Medema RH (2010) Mechanisms of centrosome separation and bipolar spindle assembly. Dev Cell 19:797-806

Tao L, Mogilner A, Civelekoglu-Scholey G, Wollman R, Evans J, Stahlberg H, Scholey JM (2006) A homotetrameric kinesin-5, KLP61F, bundles microtubules and antagonizes Ncd in

motility assays. Curr Biol 16: 2293-2302

Tucker JB, Beisson J, Roche DLJ (1980) Microtubules and control of macronuclear amitosis in *Paramecium*. J Cell Sci 44:135-151

Valentine MT, Fordyce PM, Block SM (2006) Eg5 steps it up! Cell Div 1:31

Wickstead B, Gull K, Richards TA (2010) Patterns of kinesin evolution reveal a complex ancestral eukaryote with a multifunctional cytoskeleton. BMC Evol Biol 10: 110

Wiese C, Zheng Y (2006) Microtubule nucleation: γ-tubulin and beyond. J Cell Sci 119:4143-4153

Williams NE, Williams RJ (1976) Macronuclear division with and without microtubules in *Tetrahymena*. J Cell Sci 20:61-77

Winey M, Bloom K (2012) Mitotic spindle form and function. Genetics 190: 1197-1224

Wolfe J, Hunter B, Adair WS (1976) A cytological study of micronuclear elongation during conjugation in *Tetrahymena*. Chromosoma 55: 289-308

Wu X, Xiang X, Hammer JA 3rd (2006) Motor proteins at the microtubule plus-end. Trends Cell Biol 16:135-143

Wunderlich F, Peyk D (1969) Antimitotic agents and macronuclear division of ciliates. I. Colchicine and colcemid in exponentially growing cultures of *Tetrahymena pyriformis* GL. Naturwiss 56:285-286

Wunderlich F, Speth V (1970) Antimitotic agents and macronuclear division of ciliates. IV. Reassembly of microtubules in macronuclei of *Tetrahymena* adapting to colchicine. Protoplasma 70:139-152

Xiong J, Lu Y, Feng J, Yuan D, Tian M, Chang Y, et al. (2013) *Tetrahymena* Functional Genomics Database (TetraFGD): an integrated resource for *Tetrahymena* functional genomics. Database 2013: bat008

Table I. Effect of cold treatment on cytoplasmic and Mac MTs

	Interphase cells	Division phase cells
cytoplasmic MTs	1/15	1/15
Mac MTs	0/15	15/15

Cells were incubated at 0°C for 5 min and processed for observation of MTs. Fifteen interphase cells and fifteen division phase cells were observed counted and the number of cells with cytoplasmic or Mac MTs were recorded.

Table II. Effect of nocodazole treatment on Mac division

	Mac division (%)			
	Normal	Unequal	Incomplete	Absent
DMSO (control) (n=25)	100	0	0	0
Nocodazole (n=13)	0	38	38	23

Asynchronous growing cells were treated with 30 μM nocodazole or the solvent (DMSO) for 30 min and processed for DNA staining. Cells in stage 3-5 were classified into Normal, Unequal, Incomplete, and Absent on the basis of segregation pattern of Mac DNA (see Fig.8c).

Table III. Effect of γ-tubulin depletion on Mac division

Time (h)	Mac division (%)			
	Normal	Unequal	Incomplete	Absent
0 (n=27)	100	0	0	0
12 (n=9)	100	0	0	0
14 (n=9)	67	33	0	0
17 (n=35)	9	29	14	49

cTTMGHA cells were cultured without Cd^{2+} for the time indicated, and processed for DNA staining. Cells in stage 3-5 were classified into Normal, Unequal, Incomplete, and Absent (see Fig. 8c)

Table IV. Mitotic phenotype of *KIN14A*-KO, *KIN14B*-KO and *KIN14A&14B*-KO

Strains	Normal (%)	Abnormal (%)
WT (B2086) (n=8)	100	0
KIN14A-KO-1 (n=25)	12	88
KIN14A-KO-2 (n=11)	18	82
KIN14B-KO-1 (n=17)	100	0
KIN14B-KO-2 (n=18)	100	0
KIN14A&14B-KO-1 (n=16)	19	81
KIN14A&14B-KO-2 (n=24)	13	87

The mitotic defect of single gene KO (*KIN14A*-KO, *KIN14B*-KO) and double gene KO (*KIN14A&14B*-KO) are displayed. The cells were fixed and processed for DNA staining with DAPI. Cells were classified into Normal or Abnormal depend on their chromosome segregation (see Fig. 17).

Fig. 1. Dynamic reorganization of MTs along Mac division. Image a shows interphase, while images b–f correspond to stages 1–5 of the division phase, respectively. Images a'–f' are DAPI staining images corresponding to images a–f, respectively. Z-stack images excluding top and bottom surfaces of a cell (9 slices with 0.2 μm spacing) are shown. Arrowheads and arrows indicate MT structure organized in Mic and Mac, respectively. OP: oral primordium. Bar: 10 μm.

Fig.1

α-tubulin | DNA

Interphase

Stage 1

Stage 2

Stage 3

Stage 4

Stage 5

65
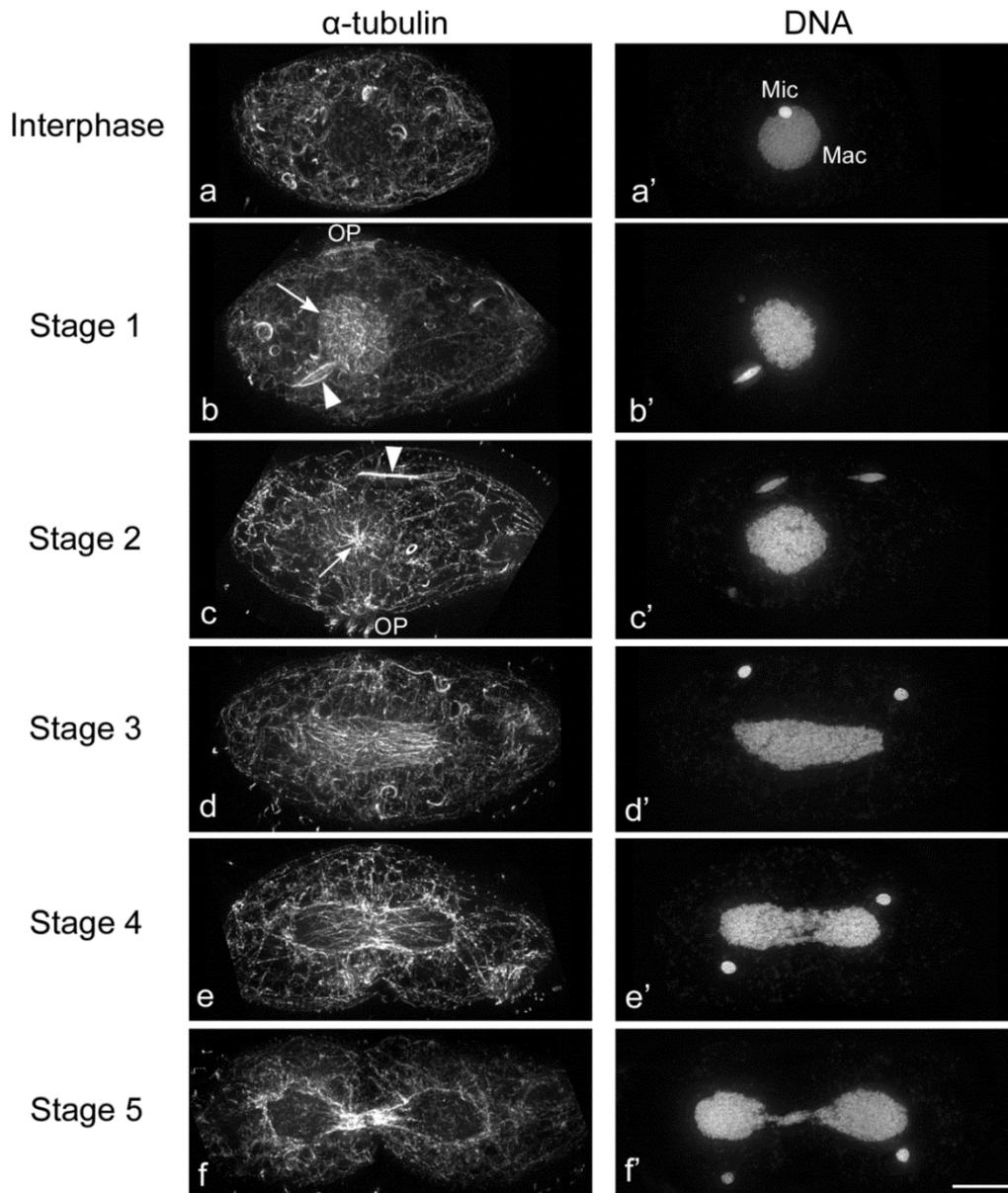
Fig. 2. Localization of γ-tubulin during mitosis. (a) Interphase Mic. γ-tubulin distributed on the surface of Mic. (b) MT bundles were suddenly formed at the beginning of mitosis (arrows). Some γ-tubulin were accumulate on spindle poles (arrowheads). (c) Complete spindle of mitosis. Accumulative signals of γ-tubulin were detectable on spindle poles (arrowheads) while many of γ-tubulin were left in the middle of spindle MTs. Arrows: inter-polar MT bundles. Yellow arrowhead: k-fiber-like MT bundle. (d) Early anaphase. γ-tubulin appeared on the middle of spindle MTs (arrowheads). (e) Late anaphase. γ-tubulin distributed on the surface of daughter nuclei (arrowheads). Bar: 5 μm

Fig.2

DNA

α-tubulin

γ-tubulin

Merged
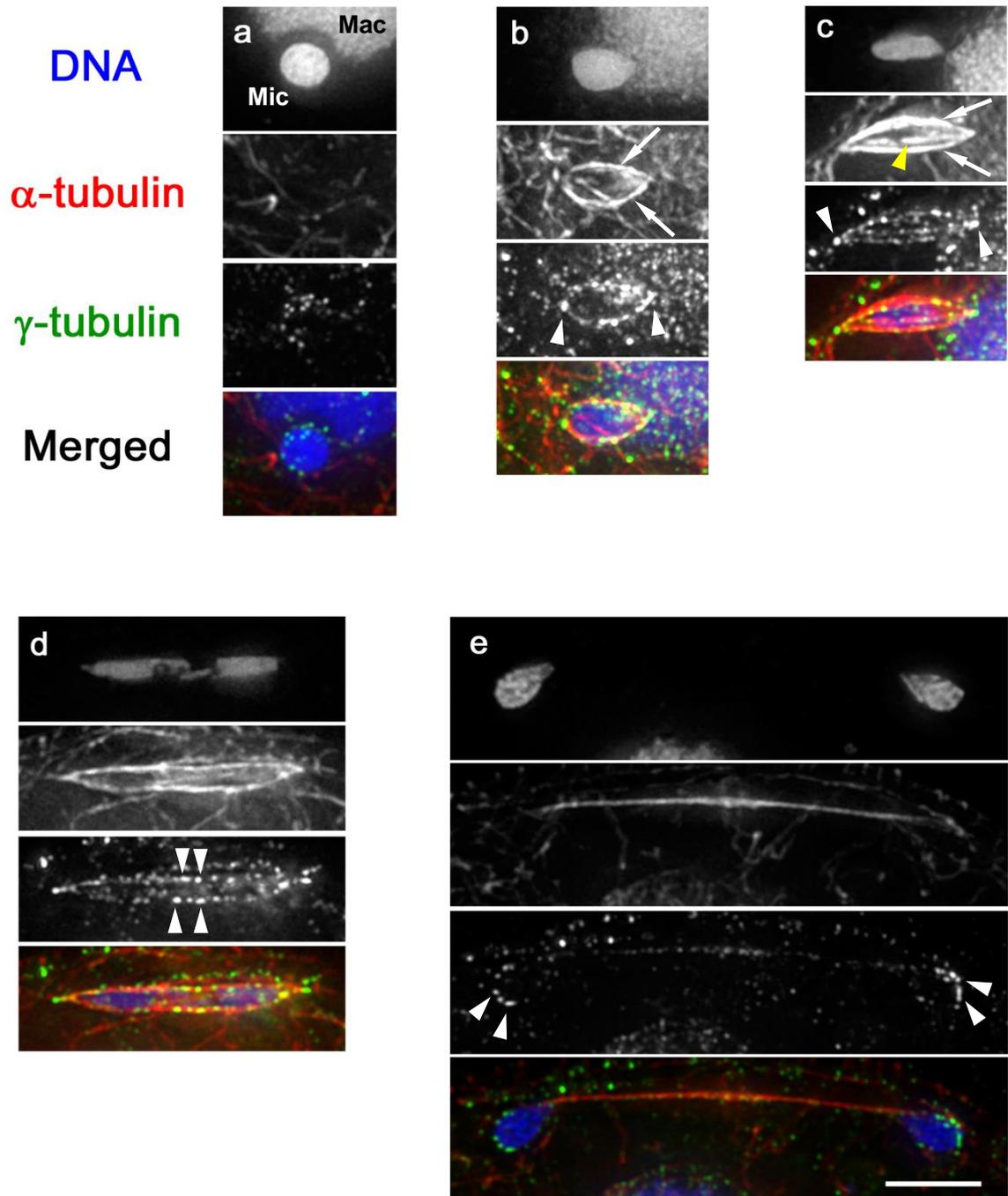
Fig. 3. Mac MTs are more stable than cytoplasmic MTs. Cells were incubated at 0°C for 5 min and processed for observation of MTs. An interphase cell (left) and a stage 2, early division phase cell (right) are shown. Z-stack images excluding top and bottom surfaces of a cell (6 slices with 0.2 µm spacing) are shown. Arrow indicates MTs remaining in Mac. Bar: 10 µm.

Fig.3

	Interphase	Division phase
α-tubulin		
DNA		
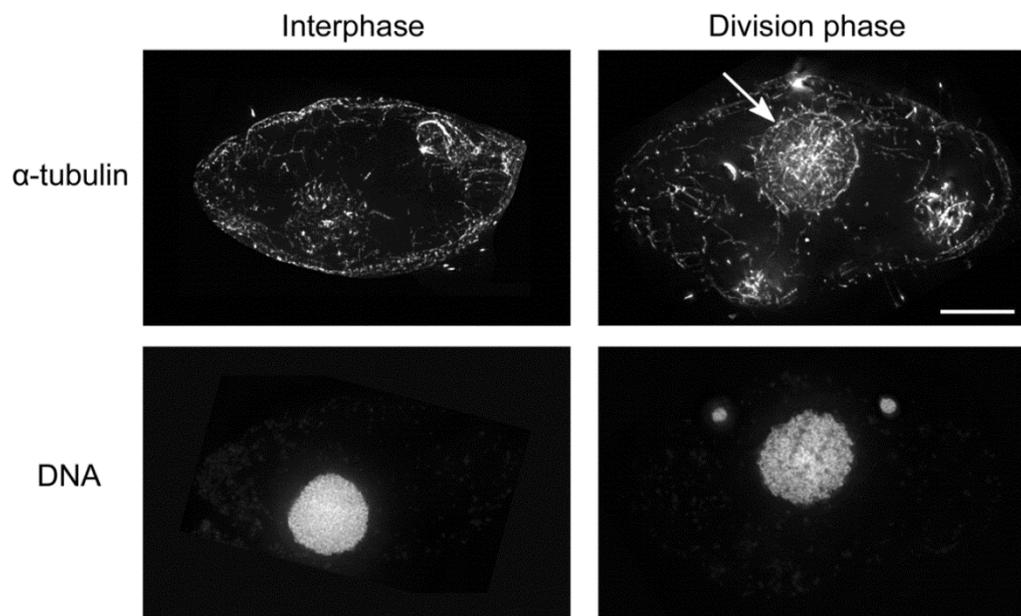
Fig. 4. Mac DNA forms numerous small particles in the division phase. Single slice image of the center of the Mac taken with a deconvolution microscope system. Bar: 5 μm.

Fig.4

	α-tubulin	DNA

Interphase

Division phase
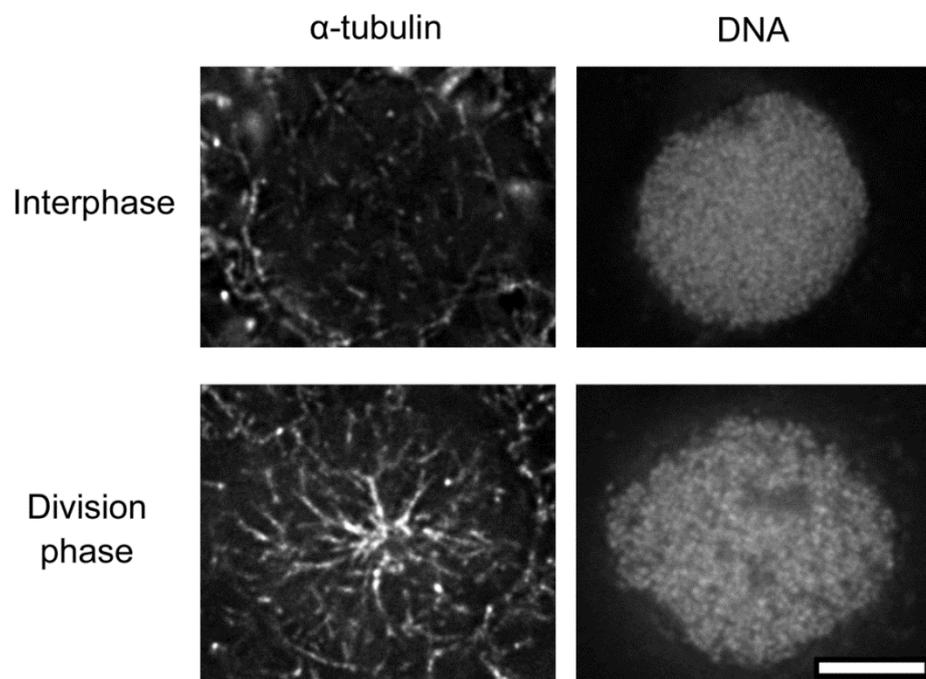
Fig. 5. Nocodazole treatment destroys Mac MTs in dividing cells. Asynchronous growing cells are treated with 30 μM nocodazole for 10 min and are processed for α-tubulin and DNA staining. Note that MTs in cytoplasm and Mac disappeared. OA and OP indicate oral apparatus and oral primordium, respectively. Bar: 10 μm.

Fig.5

α-tubulin

DNA
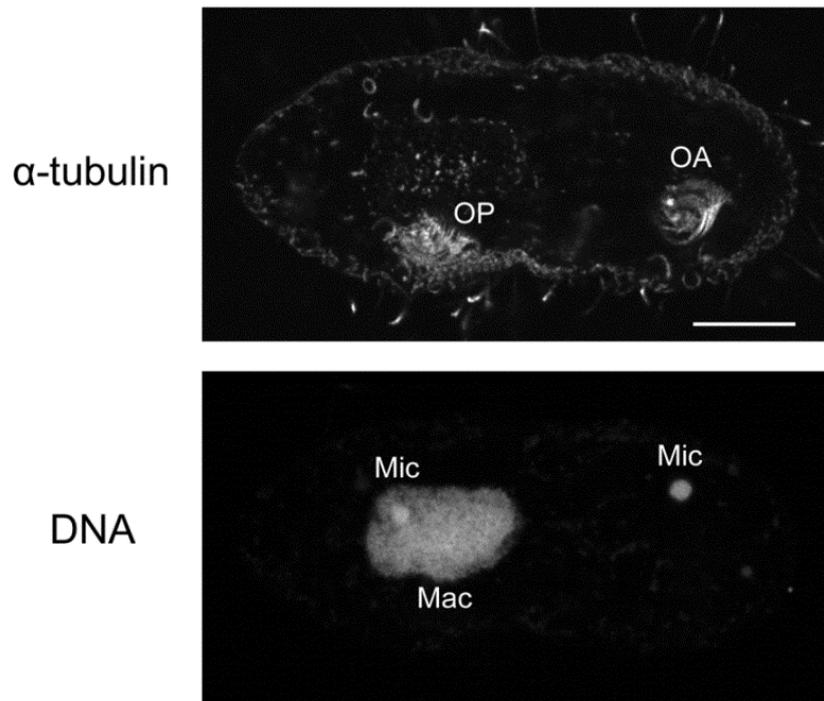
Fig. 6. Localization of γ-tubulin in dividing cells. γ-tubulin dots accumulate in the center of the Mac at stage 2 and disperse in the Mac at stages 3 and 4. In the Mic, in contrast, γ-tubulin localizes at the poles of the mitotic spindle (arrows). Z-stack images excluding top and bottom surfaces of a cell (7 slices with 0.3 μm spacing) are shown. Bar: 10 μm

Fig.6

Fig. 7. Localization of γ-tubulin in dividing cells. Single slice images corresponding to the center of the Mac before stage 2 are shown. OP: oral primordium. Bar: 5 μm.

Fig.7
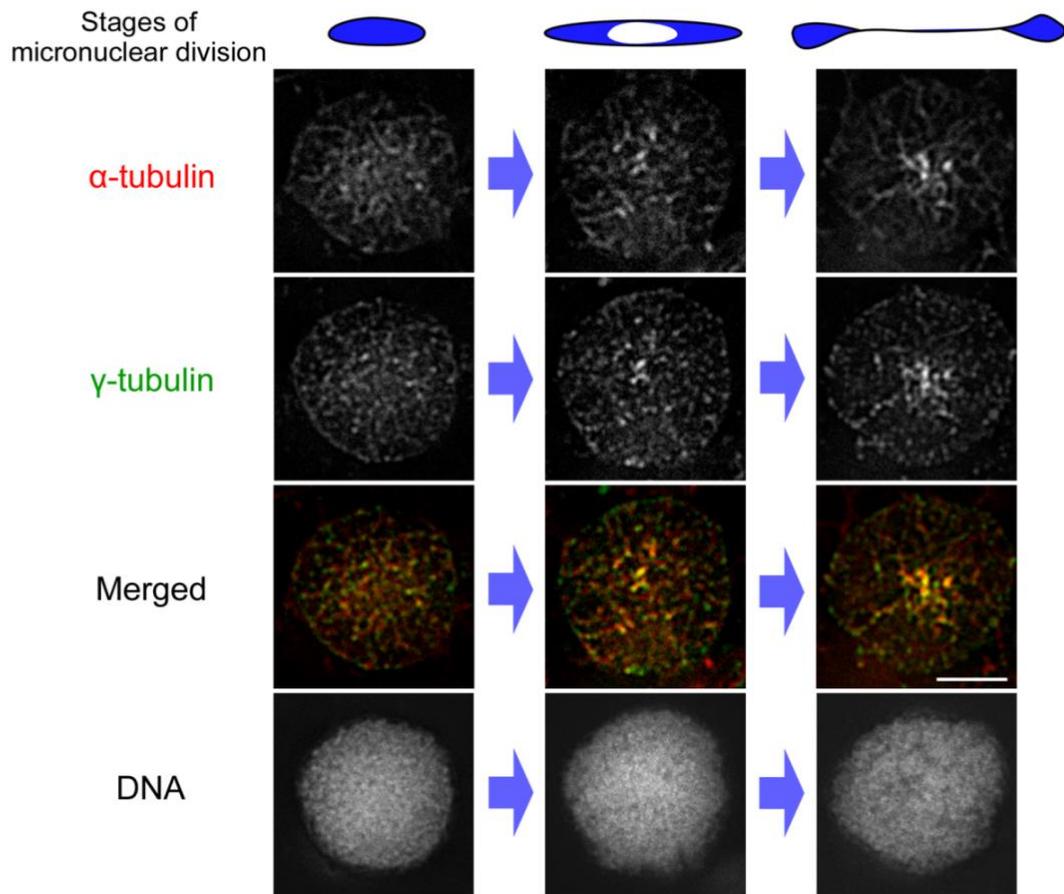
Fig. 8. γ-tubulin-mediated MT organization is required for symmetrical division of Mac.
(a) Protein expression levels of γ-tubulin in a shut-off experiment. CU428 strain, as the wild type (WT), was used for a negative control of the immunoblotting. Equal amounts of proteins were used in each lane. (b) Abnormal organization of Mac MTs is induced by the shut-off of γ-tubulin. Z-stack images at the center of the cell, including the Mac (7 slices with 0.3 μm spacing), are shown. Arrowheads and arrows indicate MT structure organized at Mic and Mac, respectively. (c) Typical DAPI staining images 17 h after Cd^{2+} washout. In 'Incomplete' cells, the Mac does not migrate to the center of each daughter cell. Note the relative position of the Mac and Mic. Bars: 10 μm.

Fig.8

a

cTTMGHA

+Cd²⁺   time (h) after Cd²⁺depletion

WT   0   25   1   2   5   9   11   14   17   21   25

GTU1-HA

α-tubulin

b

0 h   14 h   17 h

c

Normal   Unequal   Incomplete   Absent

79
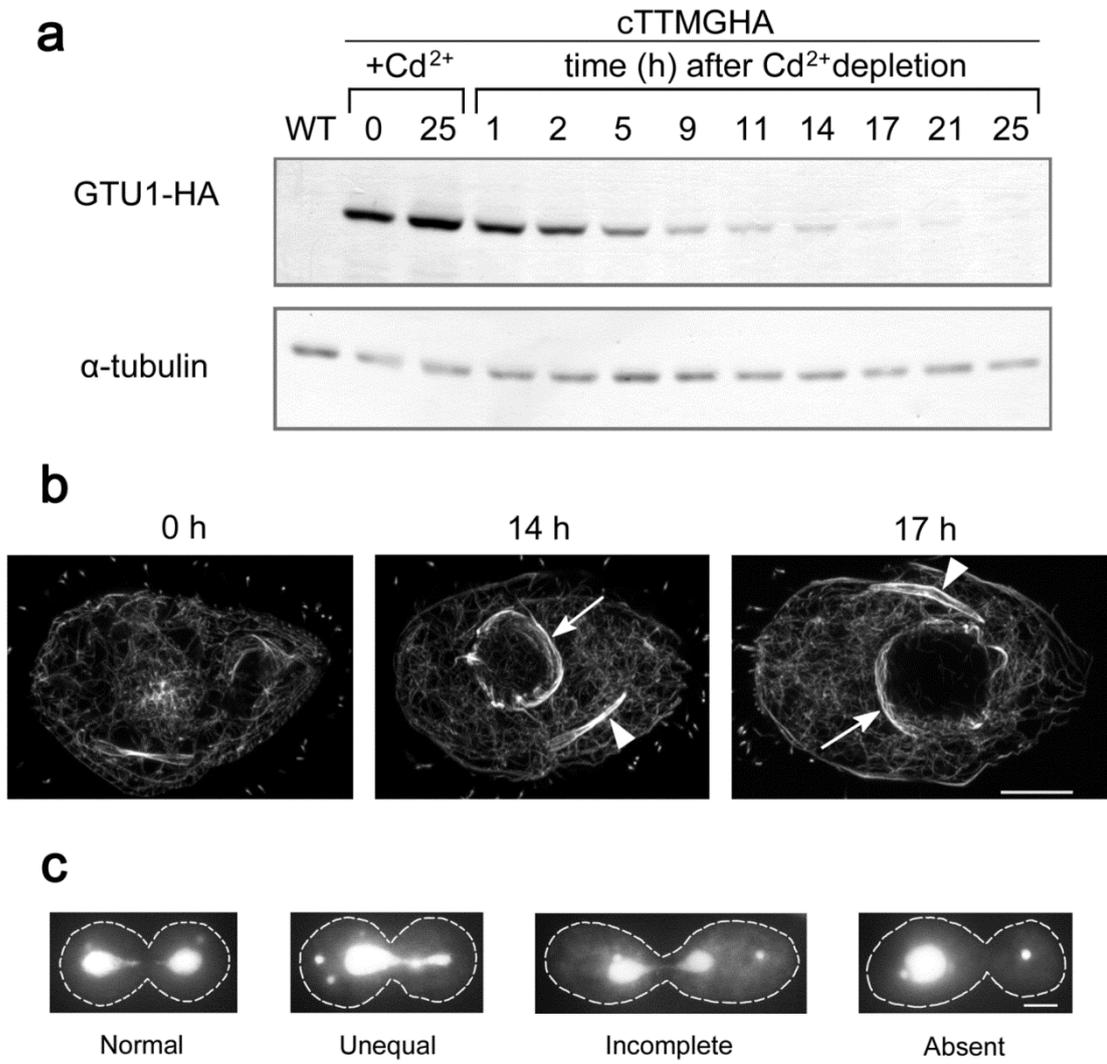
Fig. 9. Diagrams depicting the organization of MTs and γ-tubulin in the dividing Mac of *Tetrahymena*. Line can indicate either solo filament or tight bundle of MTs.

Fig.9

Stage 1

further polymerization of MTs
from the center of Mac

Stage 2

mutual sliding &
elongation of filaments
MTs penetrate minus end focusing area

Stage 3

progression of filaments bundling

Stage 4

further bundling of filemants in the
dividing region & depolymerization in
the separated area

Stage 5

packed region ?

γ-tubulin

MT

Mac envelope

81
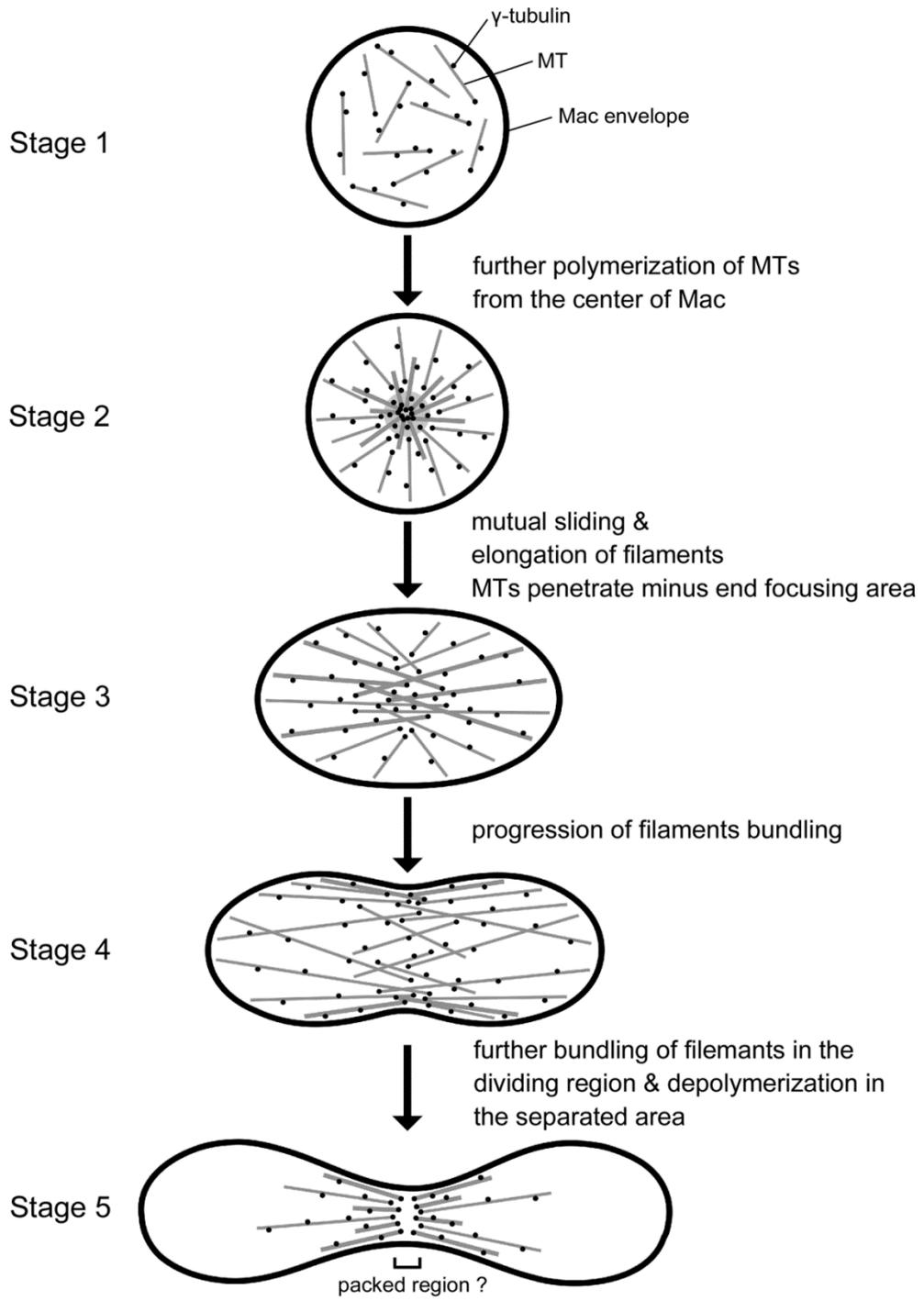
Fig. 10. Localization of DNA, MTs and γ-tubulin during elongation and shortening of crescent. Four sets of Z-stack images of each row were obtained from the same pair of cells in the same focal plane. (a) Early prophase of meiosis I. The signal of γ-tubulin is detectable (arrowhead). (b)   The beginning of elongation of crescent. γ-tubulin was accumulated on one end of crescent (arrowhead) and MTs were polymerized from there (arrow). (c) Half elongated crescent. The accumulation of γ-tubulin was decreased compared to previous stage (arrowhead). (d) Full-length crescent. MT bundles become about twice long of cell body (arrow). γ-tubulin is dispersed along   crescent (second right panel). (e) The beginning of the shortening of crescent. When chromosome condense (asterisk), MTs started to bundle together (arrow) and γ-tubulin is accumulate on the thick MT bundles. (f) The middle period of crescent shortening. γ-tubulin (arrowhead) was clearly accumulated at the end of MT bundle (arrow). Scale bar: 10μm (applicable for a to f). (f') Enlarged image of marked area in f. Single focus image is shown. γ-tubulin accumulated the edge of MT bundle. Scale bar: 4μm.

Fig.10
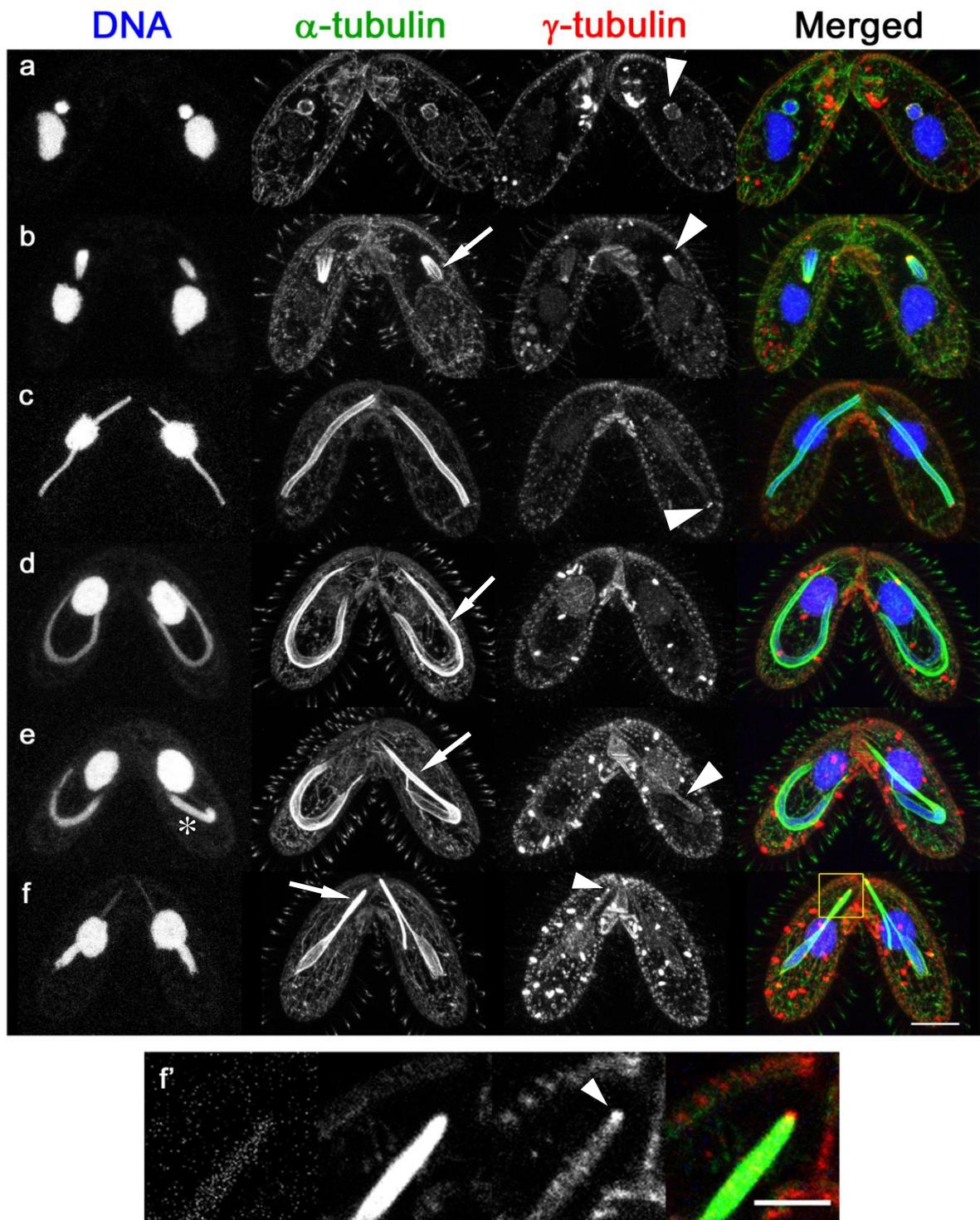
Fig. 11. Localization of DNA, MTs and γ-tubulin during meiosis I and II. (a) The Late period of crescent shortening. γ-tubulin can be clearly detected on both end of bundled MTs (arrowheads). (b) Metaphase spindle of meiosis I. γ-tubulin was accumulated on both spindle poles (arrowheads). (c and d) Anaphase of meiosis I. γ-tubulin is detectable on both of daughter nuclei (arrowheads). (e) Metaphase of meiosis II. As in the meiosis I, γ-tubulin localized on spindle poles. Scale bar: 10μm (applicable for a to e).

Fig.11
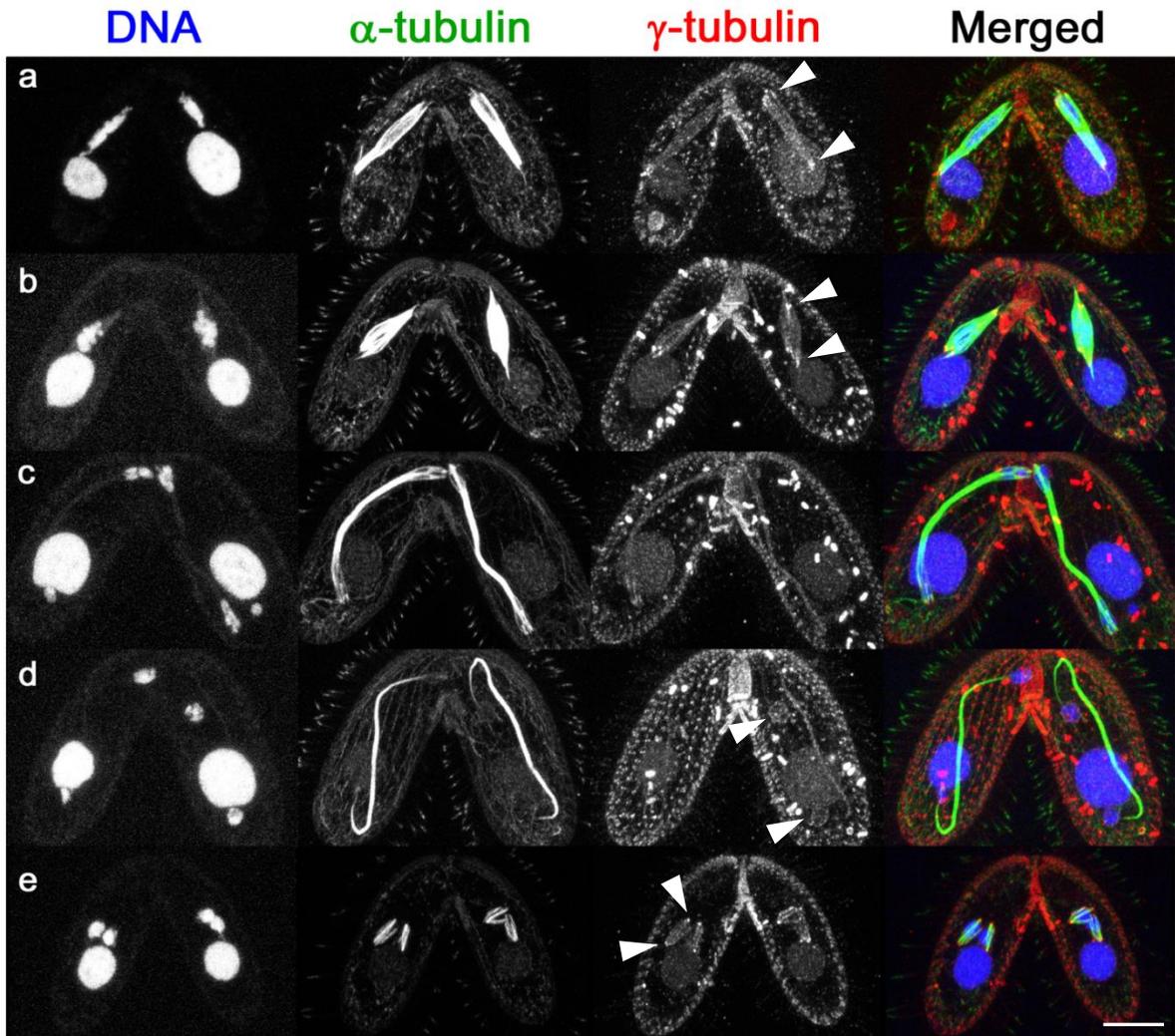
Fig. 12. Localization of DNA, MTs and γ-tubulin during gametogenic mitosis, pronuclear migration, pronuclear exchange and fertilization. (A) Anaphase of meiosis II. γ-tubulin is detectable around four daughter nuclei (arrowheads). (B) Nuclear selection. γ-tubulin is selectively accumulated on single meiotic product attached on cell junction (arrowheads) and produces astral MTs (arrows). (C) Early anaphase of gametogenic mitosis. γ-tubulin (arrowheads) distributes on whole spindle-shaped MTs (arrows). (D) Late anaphase of gametogenic mitosis. γ-tubulin was accumulate on both of daughter pronuclei (arrowheads) while they were connected by spindle (arrow). Astral MTs were polymerized from anterior pronuclei (small arrowhead). (E) Pronuclear exchange. Astral MTs (arrow) were polymerized from posterior pronucleus (arrowhead) migrating to anterior side. Small arrowhead: MT from anterior pronucleus. (F) After pronuclear exchange. γ-tubulin distributed on both of pronuclei (arrowheads) and cell junction (asterisk). Small arrowheads: MTs around pronuclei. (G) Fertilization. Whole spindle-shaped zygotic nucleus (arrow) is labelled with γ-tubulin (arrowhead). Scale bar: 10µm (applicable for A to G). (H) Enlarged image of marked area in E. Single focus image is shown. γ-tubulin accumulated on 'basket' (arrowhead) polymerized astral MT (arrow). Scale bar: 8µm.

Fig.12
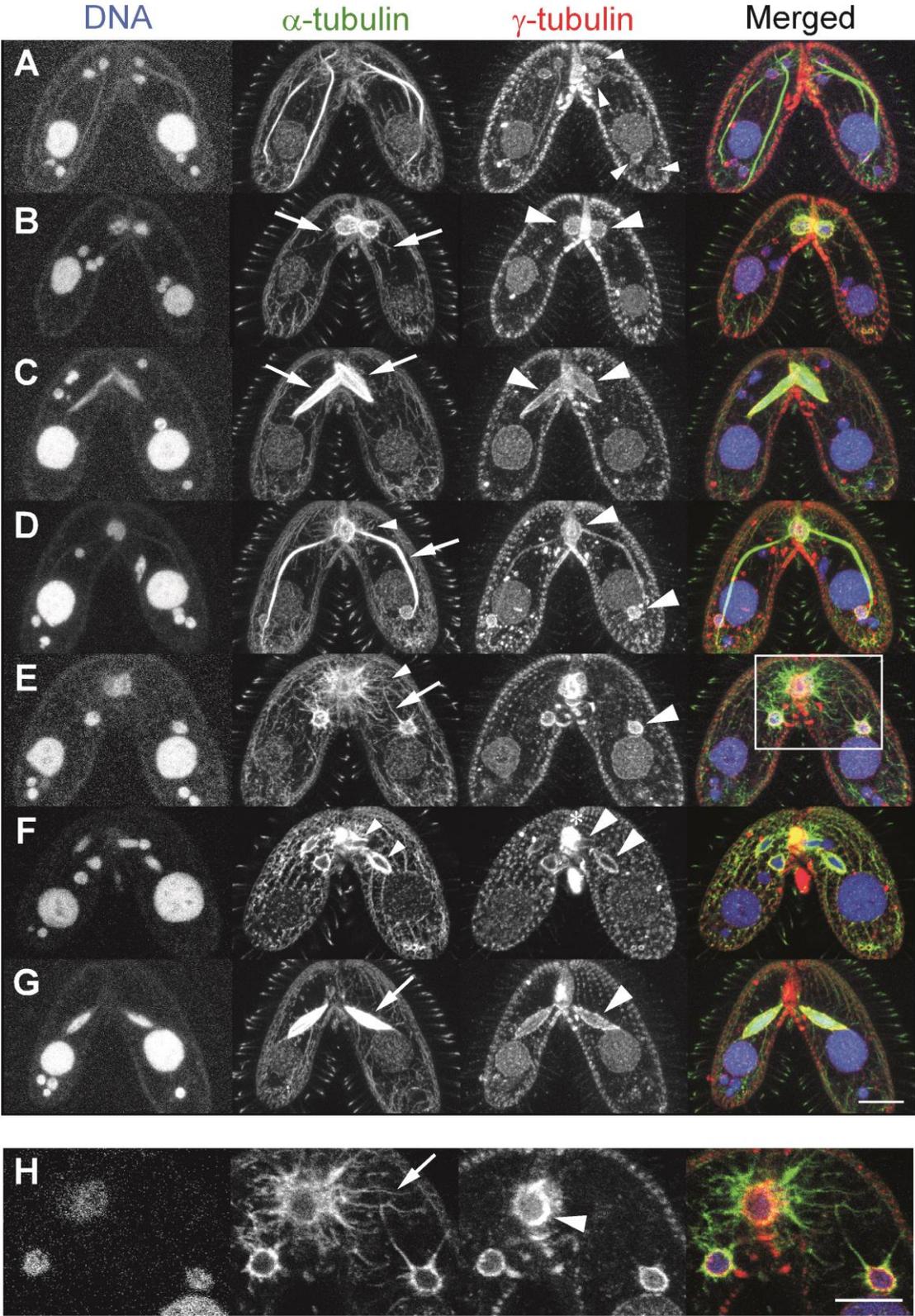
Fig. 13. Localization of DNA, MTs and γ-tubulin during post-zygotic divisions and new Mac development. (A) Early anaphase of 1st post-zygotic division. γ-tubulin (arrowhead) localized on whole spindle-shaped MTs. (B) Late anaphase of 1st post-zygotic division. Two daughter nuclei were labelled with γ-tubulin (arrowheads). (C) After 1st post-zygotic division. Two daughter nuclei (arrowheads) came closer while spindle MTs were remained (arrow). Some MTs were formed around daughter nuclei (small arrowheads). (D) Anaphase of 2nd post-zygotic division. The signal of γ-tubulin was reduced (arrow). (E) After 2nd post-zygotic division. γ-tubulin was detectable in new Macs (small arrowheads) and parental Mac (arrow). Scattered MTs were formed in paretal Mac (arrowhead). (F) Rearrangement of nuclear position. γ-tubulin was disappeared from parental Mac (arrow) accompanied with chromosome condensation. New Macs were labelled with γ-tubulin (arrowheads). (G) The characteristic pattern of nuclear position at the end of conjugation. The signal of γ-tubulin in new Macs (arrowheads) was increased. Scale bar: 10μm (applicable for A to G). (H) Enlarged image of marked area in G. Single focus image is shown. γ-tubulin polymerized some dotted MTs (arrowheads) in new Mac while some γ-tubulin did not colocalize with MTs (arrows). Scale bar: 4μm.

Fig.13

89
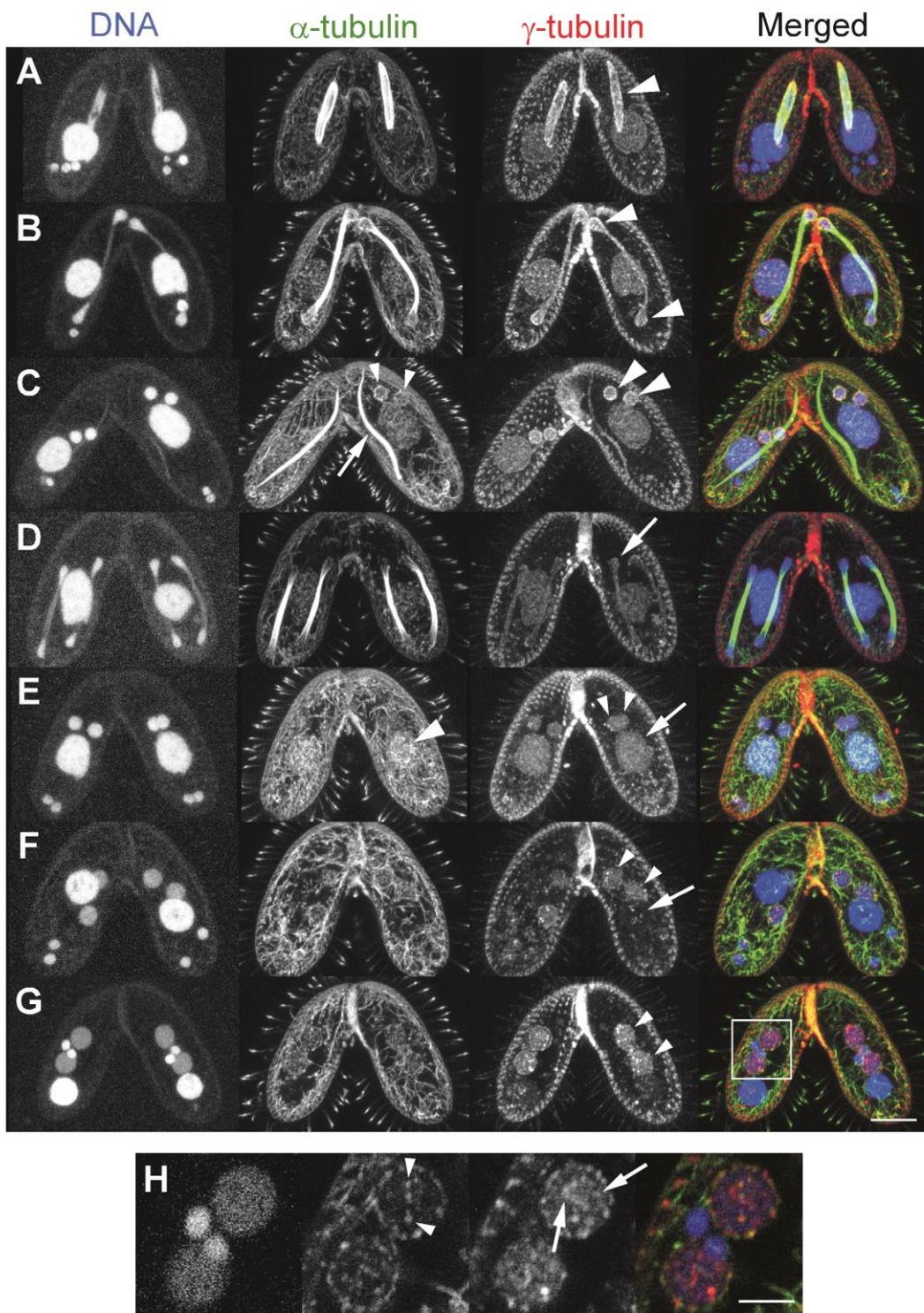
Fig.14 A phylogenetic tree of amino acid sequences of Kinesin of *Tetrahymena thermophila*, *Homo sapiens*, *Saccharomyces cerevicie*, and *Schizosaccharomyces pombe*. Bootstrap proportions >30% are shown. Each kinesin superfamily is indicated by colored box. Blue boxes show transporter kinesin superfamilies with *Tetrahymena* kinesin orthologues. Orange boxes show mitotic kinesin superfamilies with *Tetrahymena* orthologues. Kinesin 9 superfamily (purple box) is related to the regulation of motility of axoneme　[Demonchy *et al*., 2009]. Gray boxes are superfamilies without *Tetrahymena* orthologues. Scale bar indicates 0.1 substitutions at each amino acid position.

Fig.14
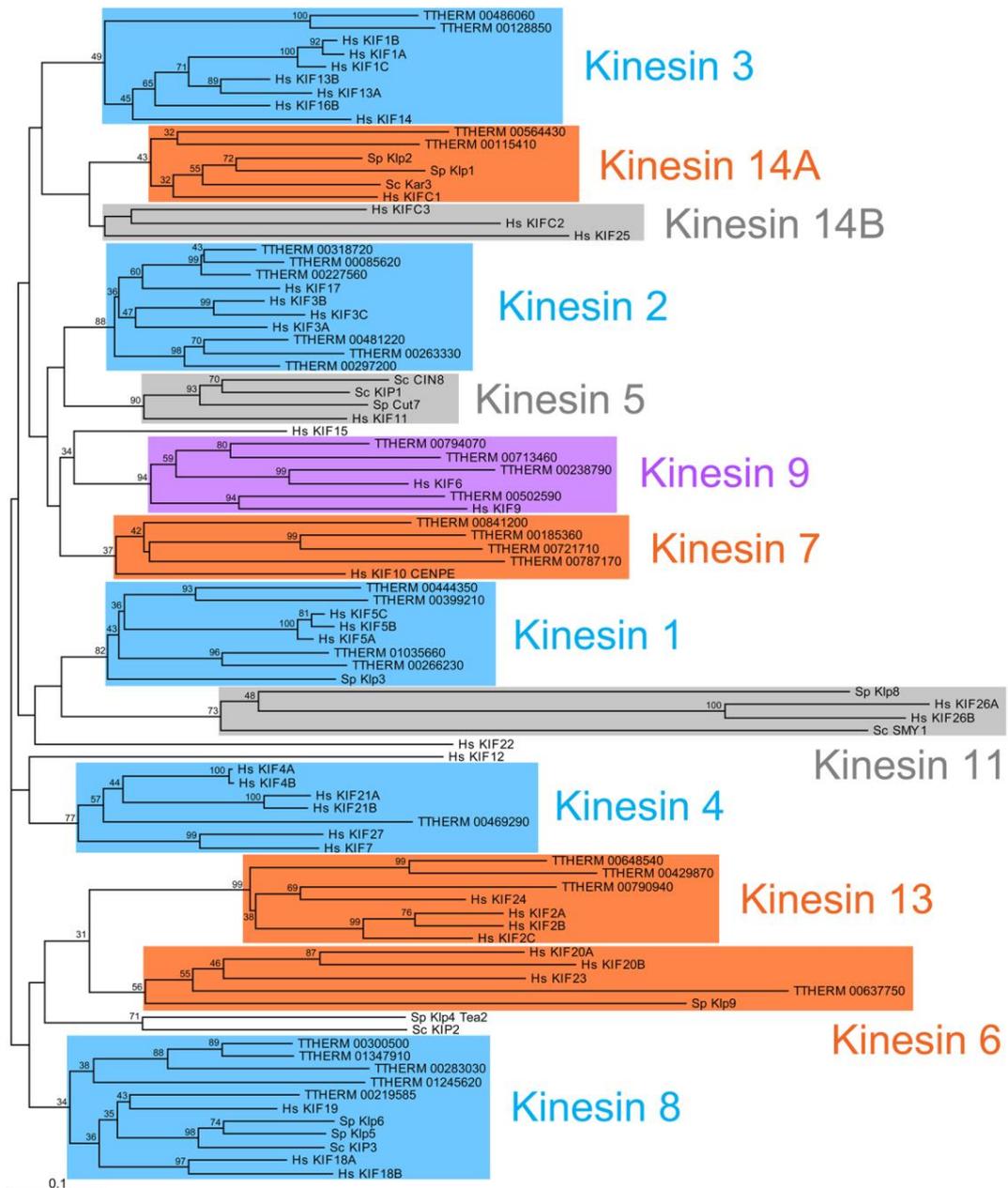
Fig.15 A phylogenetic tree of species-specific Kinesin proteins from *Tetrahymena thermophila*. Bootstrap proportions >30% are shown. Groups of kinesin which show significant similarity (>50%) are shown by gray boxes. C-kinesins are marked by orange squares. Scale bar indicates 0.1 substitutions at each amino acid position.

Fig.15
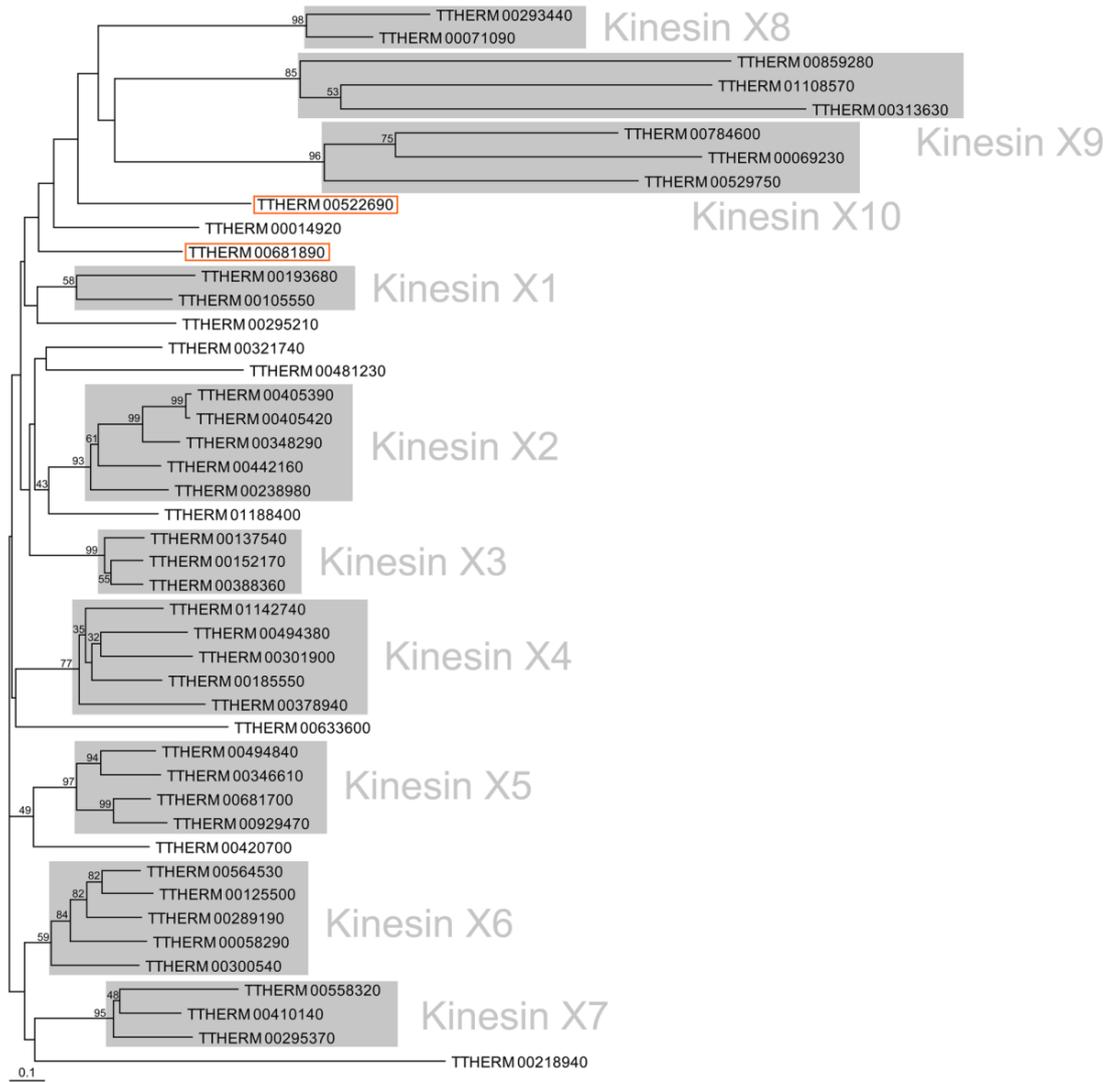
Fig. 16. The design of gene KO construct and PCR confirmation after KO experiment.
(a) Diagrams showing the strategies of gene KO of *KIN14A*, *KIN14B* and both of
KIN14A&14B. Numbered arrows showing the primers for check PCR. (b) The results of check
PCR.

Fig.16

a

b

KIN14A-Motor-KO

primer   1+4   2+4   3+4

KIN14B-Entire-KO

primer ① ② ① ② ① ②

(①: 5+7; ②: 6+7)

KIN14A & 14B-Entire-KO

primer ① ② ③ ④ ① ② ③ ④ ① ② ③ ④

(①: 8+10; ②: 9+10; ③: 5+7; ④: 6+7)

95
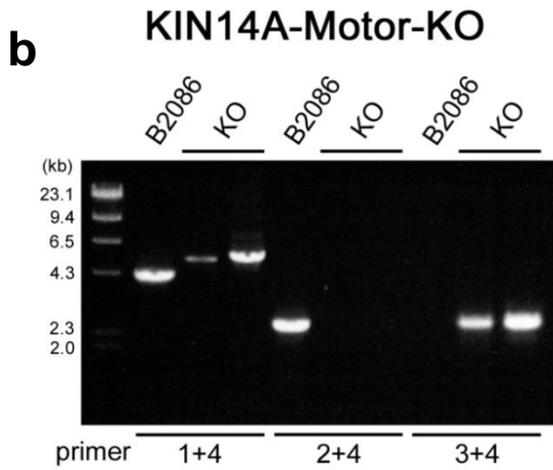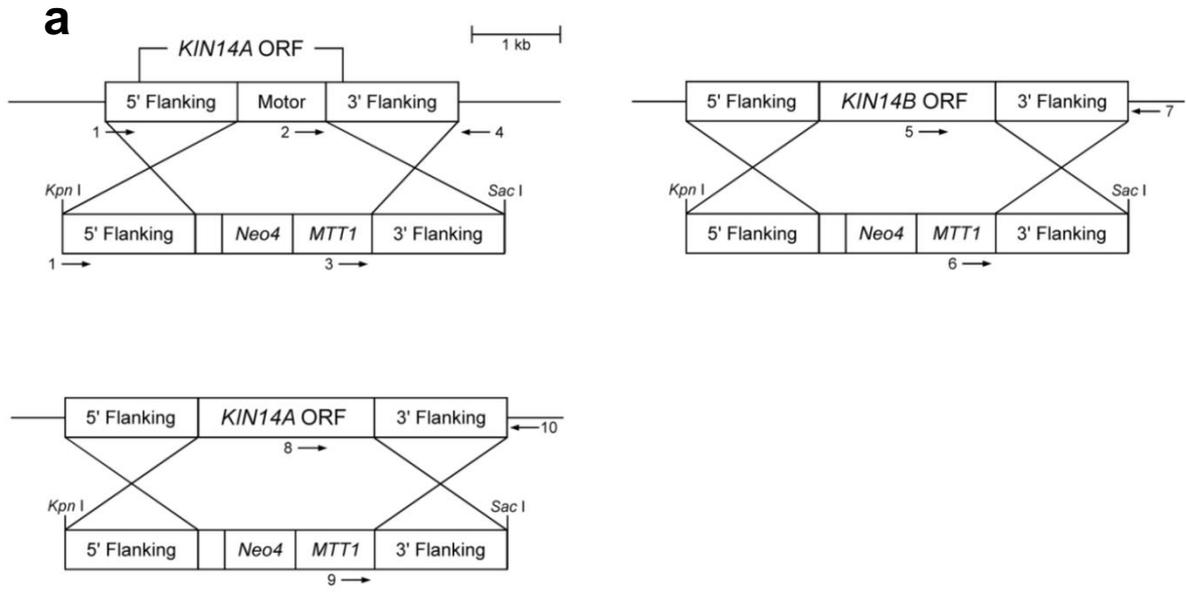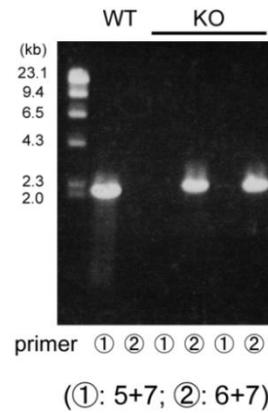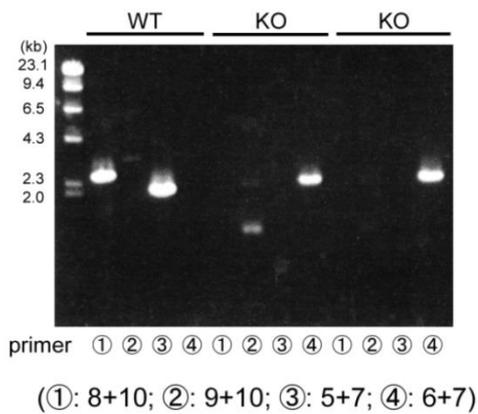
Fig. 17 Mitotic phenotype of *KIN14A*-KO. DAPI-staining image of vegetative *KIN14A*-KO cells are displayed. KIN14A is required for equal segregation during mitosis. While about <20% of the cells showed normal mitosis (left panel), mitotic chromosome segregation of most (>80%) of the cells was severely defected (Right two panels). The chromosomes were often left unsegregated at the middle of the spindle (arrowheads). Scale bar: 10 μm.

Fig.17

Normal   **Abnormal**

Fig. 18 Mitotic and amitotic phenotype of *KIN14A*-KO. DNA and MTs of vegetative *KIN14A*-KO cells are displayed. The Mic chromosomes of *KIN14A*-KO cells were often left unsegregated (arrowheads) in the middle of mitotic spindle (arrow). Scale bar: 10 µm

Fig.18
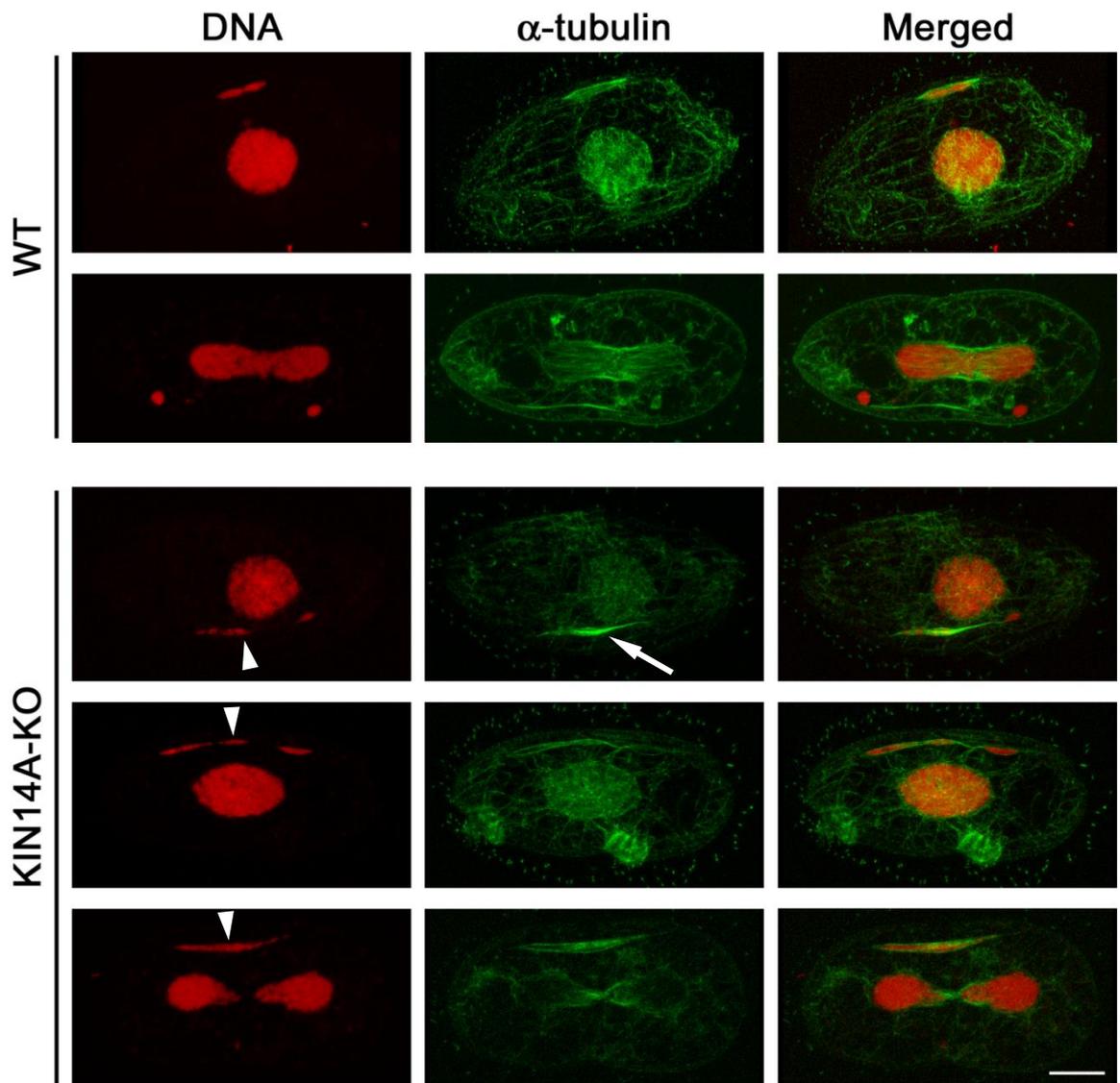
Fig. 19. Localization of KIN14A during vegetative phase. Immunofluorescence was performed on EGFP-KIN14A-overexpressing cell. Anti-GFP antibody detected the localization of KIN14A on whole mitotic spindle (arrowhead) during vegetative growth. Scale bar: 10 μm

Fig.19

DNA   **α-tubulin**   **KIN14A**   **Merged**
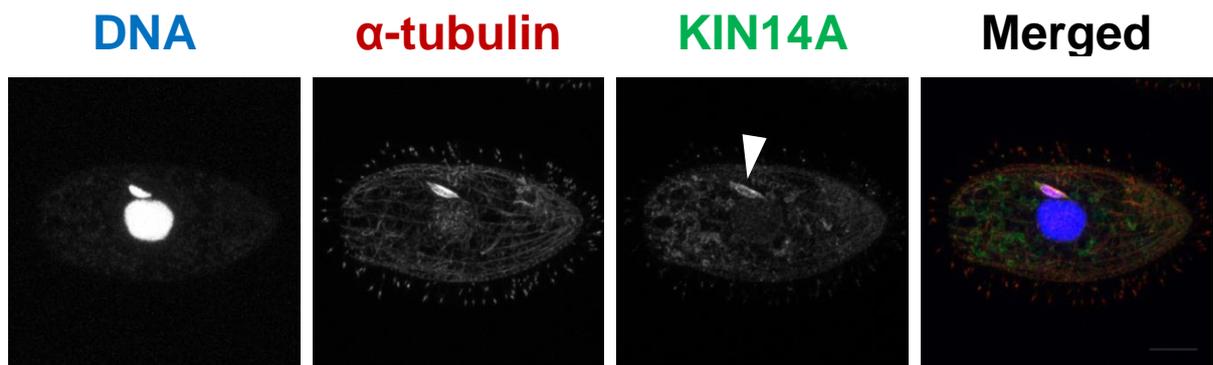
Fig. 20. Distribution of MT and DNA of wildtype cell during conjugation . (a) The beginning of the elongation of 'crescent'. (b) Fully elongated crescent. (c) The middle period of the shortening of crescent. (d) Metaphase of meiosis I. All MTs in crescent were collected to form bipolar spindle. Arrowheads: spindle poles. (e) Anaphase of meiosis I. (f) Metaphase of meiosis II. (g) Nuclear 'selection' after meiosis II. Among four meiotic products (arrowheads), one product was positioned beside the conjugation junction (yellow arrowhead). MT polymerization was detected around selected nuclei. Scale bar: 10 μm.

Fig.20

WT x WT

DNA   α-tubulin   Merged
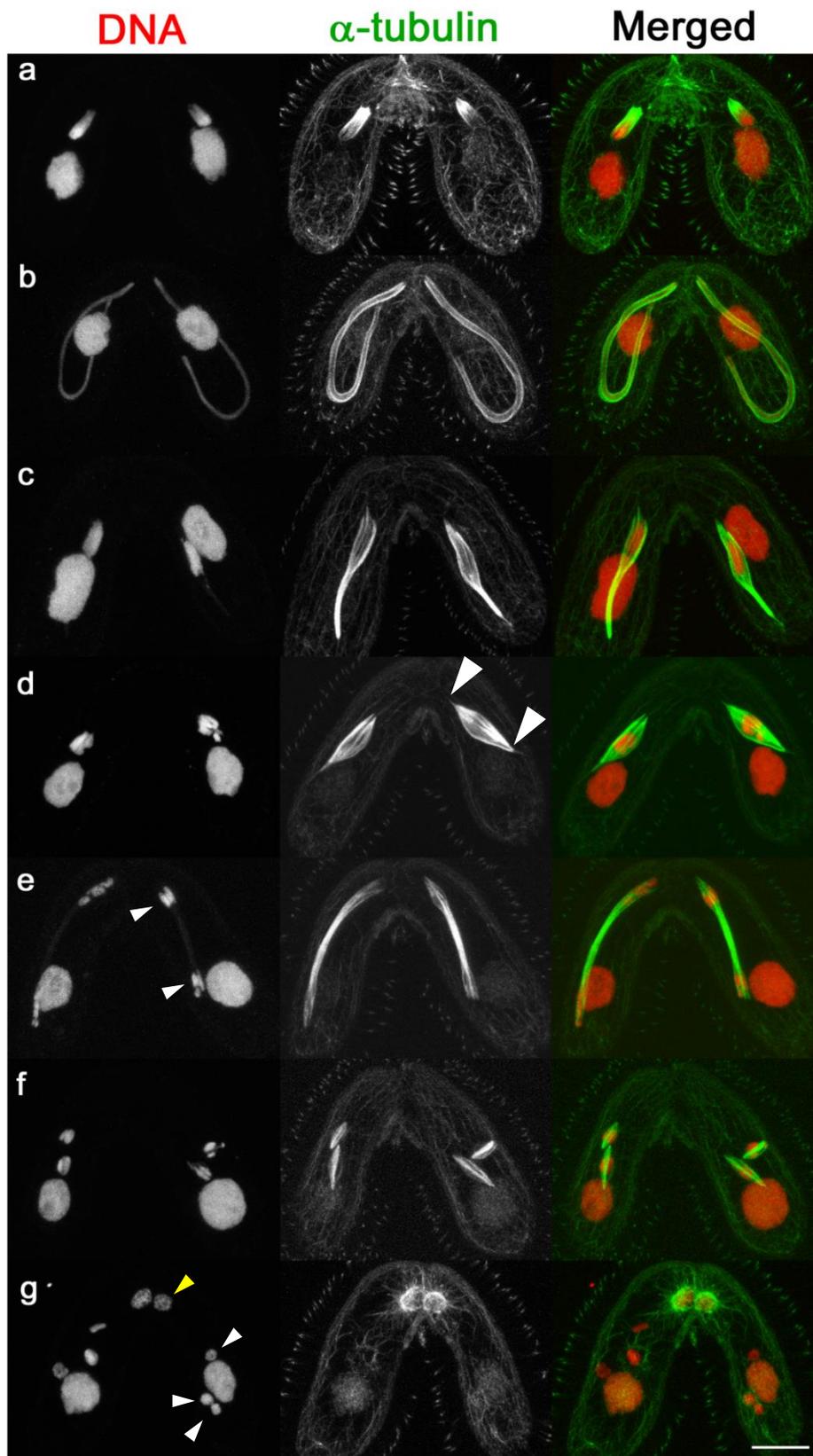
Fig. 21. **Distribution of MT and DNA of KIN14A-KO cell during conjugation** . The meiotic phenotype of the cross between KIN14A-KO cells were shown. (a) The beginning of the elongation of 'crescent'. (b) Fully elongated crescent. (c) The middle period of the shortening of crescent. (d) Metaphase of meiosis I. Compered to wildtype spindle (Fig. 20d), the ends of spindle is sharpened. (e) Inefficient chromosome segregation during meiosis I. The many of chromosomes were left in the middle of spindle (arrowheads). (f) After meiosis I. Some MTs were formed but they failed to form spindle. (g) Nuclear 'selection' after meiosis. The number of meiotic product per cell was not four (arrowheads) and the size of product was vary. Each one of products was seemed selected (yellow arrowheads). Scale bar: 10 μm.

Fig.21 KIN14AKO x KIN14AKO

DNA α-tubulin Merged
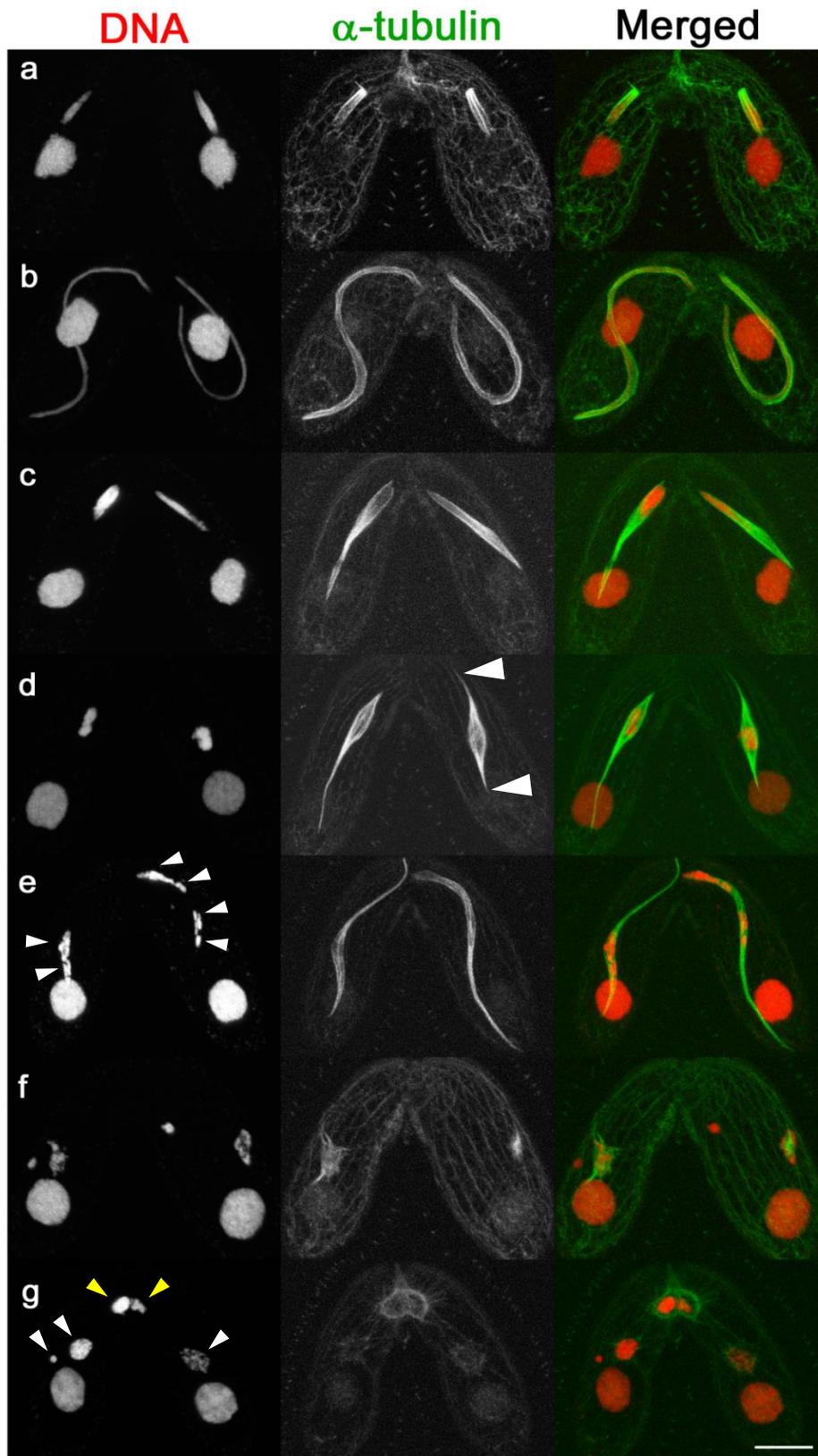
Fig. 22.   Localization of KIN14A during conjugation . The localization of KIN14A was shown. (a-d) The fluorescent signal of living EGFP-KIN14A over-producing cells. (a) During crescent shortening. KIN14A accumulated on the both ends of the crescent (arrowheads). (b) Metaphase of meiosis I. KIN14A localized on spindle poles (arrowheads). (c) Anaphase of meiosis I. (d) Metaphase of meiosis II. Scale bar: 10 µm. (e) Immuno- fluorescence of EGFP-KIN14A over-producing cells during metaphase of meiosis I. Anti-GFP antibody was used to detect KIN14A. KIN14A localized on spindle MTs near spindle poles (arrowheads). Scale bar: 10 µm.

Fig.22

EGFP-KIN14A
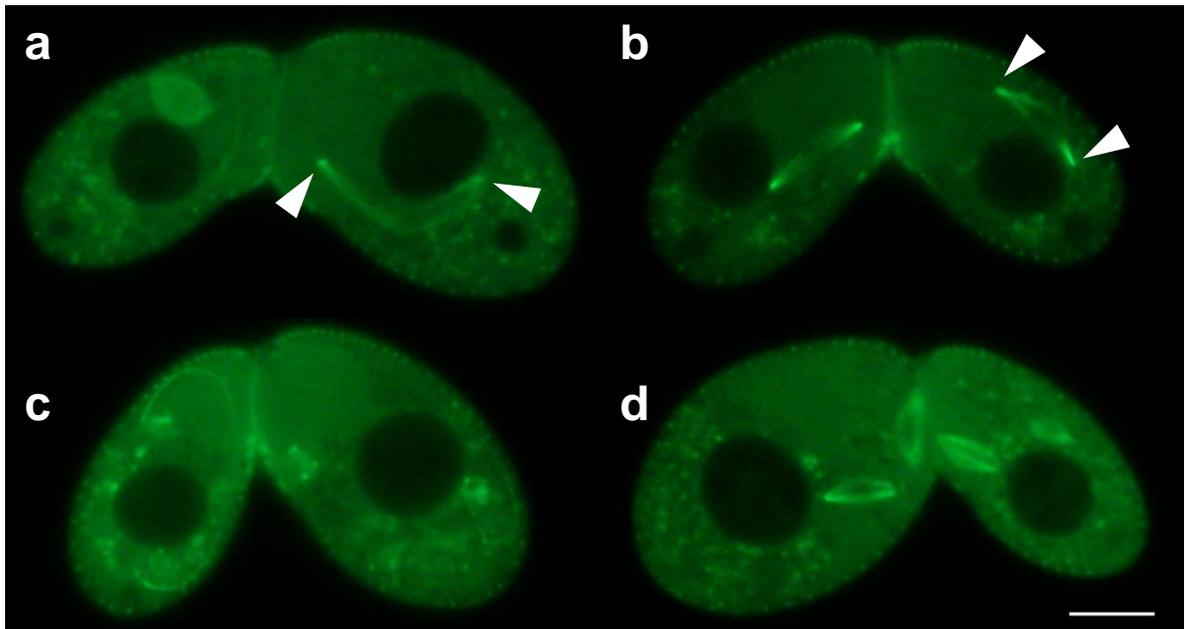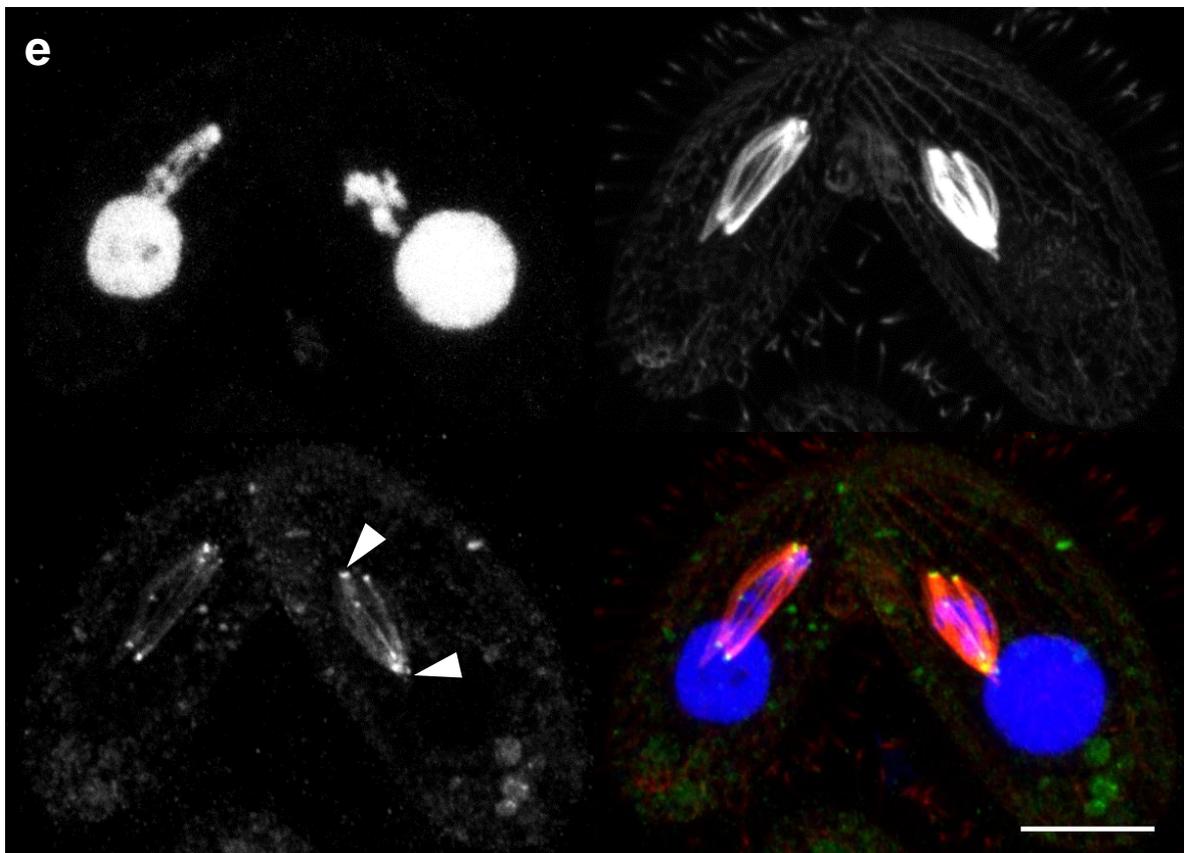
Fig. 23.   Hypothetic model of meiotic spindle formation. A model for the establishment of bipolarity of spindle during meiosis I. The cells in left side of pairs are shown.

Fig.23

DNA

γ-tubulin

Kinesin-14

Microtubule bundle